frontiers in Earth Science

ORIGINAL RESEARCH
published: 19 February 2019
doi: 10.3389/feart.2019.00012

Quantification of Basin-Floor Fan Pinchouts: Examples From the Karoo Basin, South Africa

Larissa Anne S. Hansen[1], David Mark Hodgson[1], Anna Pontén[2], Daniel Bell[3] and Stephen Flint[3]*

[1] School of Earth and Environment, University of Leeds, Leeds, United Kingdom, [2] Equinor ASA, Trondheim, Norway, [3] School of Earth and Environmental Sciences, University of Manchester, Manchester, United Kingdom

The topography of the seabed (orientation and gradient) and rheology of the flows greatly influences the character of basin-floor turbidity current deposits. Therefore, submarine fan pinchouts can help to constrain seabed topography and flow behavior at the time of deposition. Although the depositional architecture of submarine lobe pinchouts has been documented in various basin-fills, the quantification of the rates of change at pinchouts in different paleogeographic positions and basin configurations has not been attempted previously. Here, we utilize extensive outcrops and research boreholes from the oblique up-dip pinchout of Fans 3 and 4 and the lateral pinchout of Fan 3 in the Tanqua depocenter, Karoo Basin, South Africa, to compare sedimentary facies and to quantify the rates of change in gross interval thickness. At the oblique up-dip pinchout, Fan 3 thins abruptly at a rate of 12 m/km, while Fan 4 thins at a rate of 4 m/km. Marked differences between Fans 3 and 4 in sedimentary facies and architecture toward the up-dip pinchout, with termination of lobes in Fan 3 and a channel-lobe transition zone and external levee in Fan 4, suggests progradation of the system. The thinning rate of the lateral pinchout of Fan 3 is 2 m/km, with the presence of hybrid beds in the lower part of Fan 3, while the upper part is dominated by structured sandstones and thin-bedded heterolithics. The variations in facies suggest that lobe-scale frontal and lateral pinchouts are stacked at the lobe complex-scale lateral pinchout of Fan 3, highlighting the importance of a hierarchical understanding when studying basin-floor fan pinchouts. The quantified rates of change in fan thickness and sedimentology on the oblique up-dip and lateral fan pinchouts are markedly different. Contrasting pinchout architecture above slopes with subtle differences in gradient and orientation cautions against the simple definition of reservoir input parameters for stratigraphic traps in submarine fan systems.

Keywords: fan pinchout, Tanqua depocenter, hybrid beds, hierarchy, lobes

OPEN ACCESS

Edited by:
Amanda Owen,
University of Glasgow,
United Kingdom

Reviewed by:
Mattia Marini,
University of Milan, Italy
Aggeliki Georgiopoulou,
University College Dublin, Ireland

****Correspondence:***
Larissa Anne S. Hansen
l.a.hansen@leeds.ac.uk

Specialty section:
This article was submitted to Sedimentology, Stratigraphy and Diagenesis, a section of the journal Frontiers in Earth Science

Received: *10 November 2018*
Accepted: *23 January 2019*
Published: *19 February 2019*

Citation:
Hansen LAS, Hodgson DM, Pontén A, Bell D and Flint S (2019) Quantification of Basin-Floor Fan Pinchouts: Examples From the Karoo Basin, South Africa. Front. Earth Sci. 7:12. doi: 10.3389/feart.2019.00012

INTRODUCTION

Understanding the architecture and sedimentology of basin-floor fans, and their component distributive channel-fills, channel-lobe transition zones, and lobes has evolved considerably in the last 30 years due to improved seabed imaging and extensive outcrop studies (Walker, 1978; Twichell et al., 1992; Bouma and Rozman, 2000; Carr and Gardner, 2000; Dudley et al., 2000; Satur et al., 2000; Hodgson et al., 2006; Brooks et al., 2018). It is recognized that submarine lobes

exhibit diverse geometries, stacking patterns and facies distributions (Twichell et al., 1992; Bouma and Rozman, 2000; Hodgson et al., 2006; Deptuck et al., 2008; Prélat et al., 2009; Groenenberg et al., 2010), including the common occurrence of hybrid beds at lobe fringes (Haughton et al., 2009; Hodgson, 2009; Patacci et al., 2014; Porten et al., 2016; Kane et al., 2017; Pierce et al., 2018). The pinchout of basin-floor sandbodies can be used to better constrain the scale and orientation of seabed topography, and the paleogeographic configuration of basins at the time of deposition (Smith and Joseph, 2004; Bakke et al., 2013; Cobain et al., 2017; Spychala et al., 2017a,b). Interest in the architecture and facies distribution at basin-floor fan fringes, and the characteristics of fan pinchouts, have been driven by a need to improve prediction of pinchouts as stratigraphic trap targets for hydrocarbon reservoirs (Pickering, 1981; Bouma and Rozman, 2000; Etienne et al., 2012; Bakke et al., 2013; Marini et al., 2015; Nagatomo and Archer, 2015; Spychala et al., 2017b,c). Exhumed frontal and lateral basin-floor fan pinchouts have been characterized in several basins (Pickering, 1981; Rozman, 2000; Etienne et al., 2012; Nagatomo and Archer, 2015; Spychala et al., 2017b,c), but very few outcrop studies are available from (oblique) up-dip fan pinchouts (Amy et al., 2007; Brooks et al., 2018). Furthermore, quantification of the rate at which pinchout characteristics, such as thickness, sandstone content and facies variations change, is rarely constrained.

The exhumed Fans 3 and 4 systems in the Tanqua depocenter, Karoo Basin, South Africa have been the subject of various studies on their architecture (Morris et al., 2000; Johnson et al., 2001; Prélat et al., 2009), sequence stratigraphy (Hodgson et al., 2006), and deposits indicating flow transformation from the proximal to distal areas (Kane et al., 2017; Spychala et al., 2017b). The well-constrained paleogeography and excellent exposures permit a quantitative study of the oblique up-dip pinchouts of Fans 3 and 4 and lateral pinchout of Fan 3. The aim of this study is to assess the differences between oblique up-dip, lateral, and frontal lobe complex pinchouts via detailed quantification of the thickness and facies changes toward the pinchouts. Additionally, the differences in stacking patterns and architectural elements of the up-dip pinchouts of Fans 3 and 4 are described for the first time. This provides new insights into the stratigraphic evolution of the up-dip pinchouts on basin margins.

GEOLOGICAL AND STRATIGRAPHIC SETTING

The Karoo Basin is interpreted as a retroarc foreland basin that formed on the southern margin of the Gondwana paleocontinent inboard of a fold and thrust belt (De Wit and Ransome, 1992; Veevers et al., 1994; Visser and Praekelt, 1996; Visser, 1997; López-Gamundí and Rossello, 1998). Recent radiometric dating (Blewett and Phillips, 2016) and tectonostratigraphic analyses (Tankard et al., 2012, 2009) support a Triassic age for development of the Cape Fold Belt. Subsidence during the Permian pre-foreland basin stage has been attributed to dynamic topography (mantle flow) associated with the subducting plate and variable foundering of basement blocks (Pysklywec and Mitrovica, 1999; Tankard et al., 2009). The southwestern Karoo Basin is subdivided into the Laingsburg and Tanqua depocenters (**Figure 1A**). The basin-fill comprises the Late Carboniferous to Early Jurassic Karoo Supergroup, which stratigraphically comprises the glacial Dwyka Group, the deep-marine to shallow-marine Ecca Group and non-marine (fluvial) Beaufort Group (Smith, 1990). The Ecca Group is an approximately 1,400 m thick shallowing upward succession of sediments from deep-water to fluvial settings (Hodgson, 2009; King et al., 2009; Flint et al., 2011). Part of the Ecca Group is the ca. 400 m thick progradational Skoorsteenberg Formation, which comprises four submarine fans (Fans 1 to 4) and an overlying base-of-slope to lower slope succession termed Unit 5 (Bouma and Wickens, 1994; Morris et al., 2000; Johnson et al., 2001; Hodgson et al., 2006; Wild et al., 2009) (**Figure 1B**). The stratigraphic framework of the Tanqua depocenter is constrained by several field studies (Bouma and Wickens, 1991; Johnson et al., 2001; Hodgson et al., 2006; Prélat et al., 2009; Kane et al., 2017) and 11 research boreholes (Luthi et al., 2006; Hofstra et al., 2017; Spychala et al., 2017b). Fans 1 to 4 are sandstone-rich and up to 65 m thick (Johnson et al., 2001) with each fan interpreted to represent a lowstand systems tract, and with the intervening fine-grained deposits of regional extent representing the related transgressive and highstand systems tracts (Goldhammer et al., 2000; Johnson et al., 2001; Hodgson et al., 2006). Paleocurrents and thickness distributions suggest that Fans 1 to 3 were point sourced from the SW, whereas Fan 4 was sourced from both the SW and W (Dudley et al., 2000; Wickens and Bouma, 2000; Hodgson et al., 2006; Spychala et al., 2017b). This study focuses on the oblique up-dip pinchouts of Fans 3 and 4 in the Klein Hangklip area and the lateral pinchout of Fan 3 only in the Gemsbok valley area (**Figure 2**).

METHODOLOGY AND DATA SET

For this study, 39 sedimentological logs were collected around the Klein Hangklip and Gemsbok valley areas (**Figure 2**). The Gemsbok valley area logs compliment those of Prélat et al. (2009), whereas the Klein Hangklip area logs for Fans 3 and 4 are new to this study, although some of the area overlaps with Cobain et al. (2017) who focussed on injectites below Fan 3. Sedimentary logs from Fans 3 and 4 from five cored research boreholes (OR1, NS4, NB2, GBE01, NS2) (Hodgson, 2009; Kane et al., 2017) were utilized. Sedimentary logs record data on lithology, paleocurrents, sedimentary structures and bed thickness. Logs were collected at 1:25 scale in the field. The base of Fan 4 was used as a datum in all correlation panels. Paleocurrent measurements from previous studies (Hodgson et al., 2006; Prélat et al., 2009; Spychala et al., 2017b) were supplemented by 241 measurements from this study collected from current-ripple laminated sandstones, and flute and groove casts on the bases of sandstone beds.

The isopach thickness map of Fan 3 is constrained by 68 thickness measurements, partly utilizing data from previous studies (Hodgson et al., 2006; Prélat et al., 2009; Hofstra et al., 2015). The map was generated in ArcGIS using the Spatial

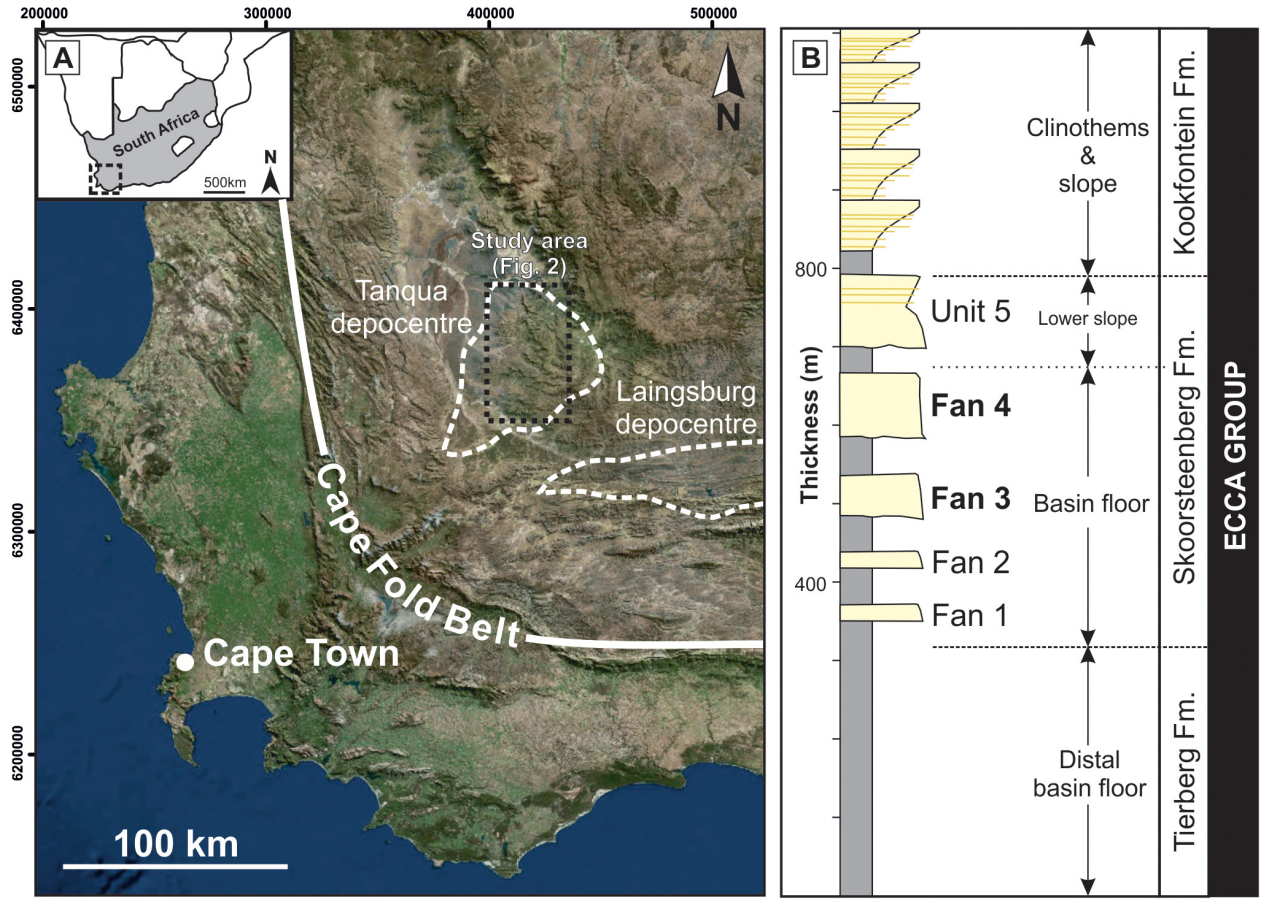

FIGURE 1 | (A) Location map of the Karoo Basin and the Tanqua and Laingsburg depocenters inboard of the Cape Fold Belt. The Tanqua depocenter is the focus of this study. **(B)** Stratigraphic column of the Tanqua depocenter (redrawn after Prélat et al., 2009; Hofstra et al., 2015). This study focuses on Fans 3 and 4 of the Skoorsteenberg Formation. Image taken from ArcMap: Esri, DigitalGlobe, GeoEye, Earthstar Geographics, CNES/Airbus DS, USDA, USGS, AeroGRID, IGN, and the GIS User Community.

Analyst tool, using the kriging interpolation method due to the directional bias in the dataset. Kriging assumes that the distance or direction between sample points reflects a spatial correlation that can be used to explain variation in the surface (Oliver, 1990).

SEDIMENTARY FACIES AND DEPOSITIONAL ENVIRONMENTS

Nine sedimentary facies are summarized in **Table 1** and **Figure 3**, and are grouped into four depositional environments. The depositional environments are distinguished by their constituent facies, geometries and paleogeographic context. The depositional environments, and their spatial and stratigraphic context, builds on extensive previous studies in the Tanqua depocenter (Johnson et al., 2001; Sullivan et al., 2004; Hodgson et al., 2006; Luthi et al., 2006; Prélat et al., 2009), and through comparison to depositional environments from slope-to-basin-floor systems mapped in the adjacent Laingsburg depocenter (e.g., Hodgson et al., 2011; Van der Merwe et al., 2014; Morris et al., 2016; Brooks et al., 2018).

Channel-Fills

Submarine channels form pathways for sediment transport and occur on the slope, base-of-slope and proximal to medial parts of basin-floor fan systems (Walker, 1978; Carr and Gardner, 2000; Johnson et al., 2001). In the Tanqua depocenter, channel-fills have lenticular geometries, are typically sand-rich, and vary from incised channel-fills (10–15 m deep) at the base of slope (Hodgetts et al., 2004; Sullivan et al., 2004; Luthi et al., 2006; Hofstra et al., 2017) to distributary channel-fills (2–6 m deep) of the middle to distal fan (Johnson et al., 2001; Hodgson et al., 2006). The channel-fills are more closely spaced at the base of slope, and form a distributive pattern across the middle and distal parts of the fan (Johnson et al., 2001; Hodgetts et al., 2004; Hodgson et al., 2006).

External Levees

External levees are defined as wedge-shaped deposits that confine channels and are composed of thin-bedded siltstones and sandstones (Kane et al., 2007; Kane and Hodgson, 2011; Morris et al., 2014; Hansen et al., 2015), with high proportions

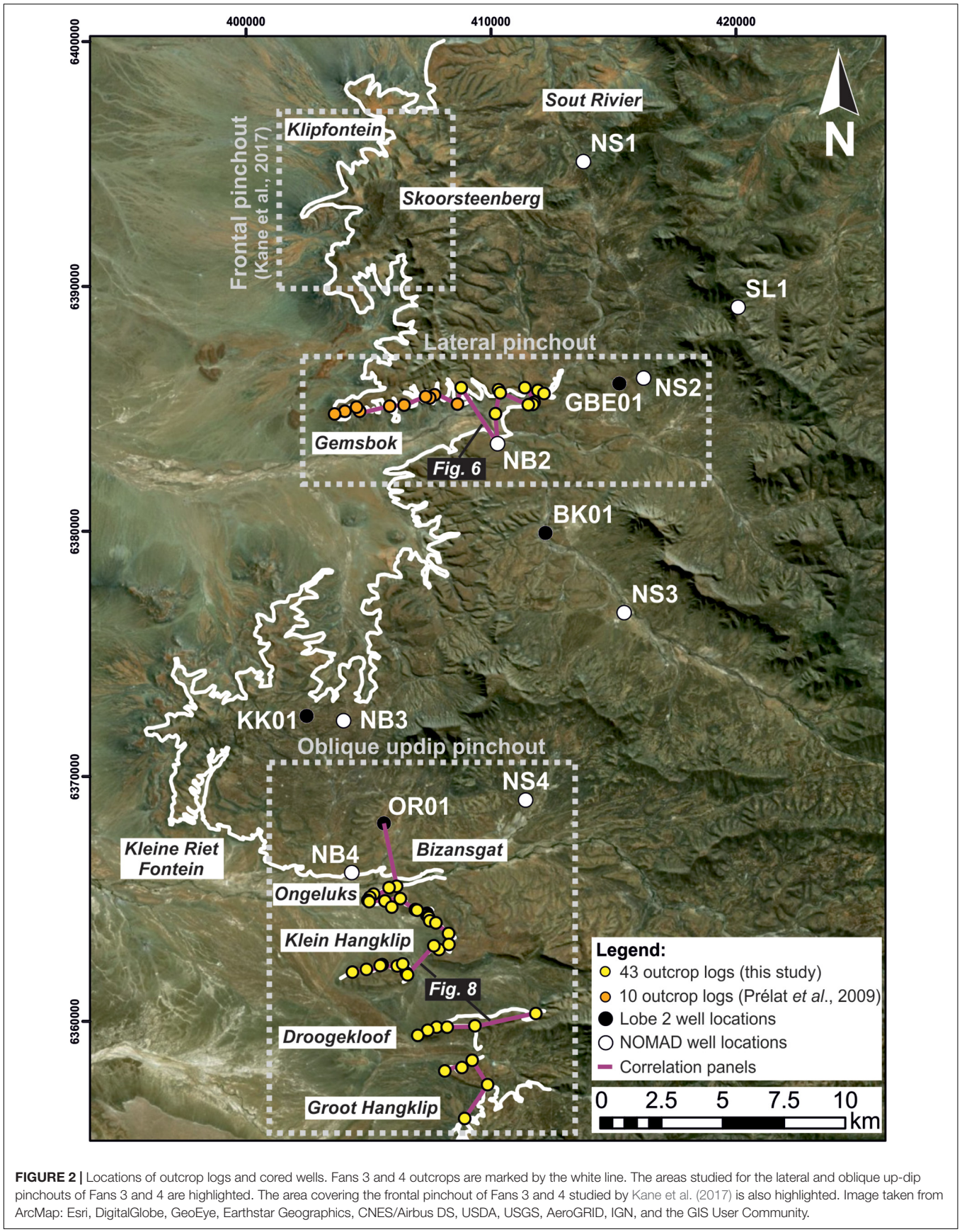

FIGURE 2 | Locations of outcrop logs and cored wells. Fans 3 and 4 outcrops are marked by the white line. The areas studied for the lateral and oblique up-dip pinchouts of Fans 3 and 4 are highlighted. The area covering the frontal pinchout of Fans 3 and 4 studied by Kane et al. (2017) is also highlighted. Image taken from ArcMap: Esri, DigitalGlobe, GeoEye, Earthstar Geographics, CNES/Airbus DS, USDA, USGS, AeroGRID, IGN, and the GIS User Community.

TABLE 1 | Observed sedimentary facies, their process interpretation and depositional environment.

Sedimentary facies	Grain size	Thickness range	Description	Process interpretation	Depositional environment
Structureless sandstone (F1)	fs to vfs	Beds 0.2–4 m thick	Sharp, erosional or loaded base; common flute and tool marks and dewatering structures; form high amalgamation units; up to 10% mudclasts	Deposited by high-density turbidity currents (Lowe, 1982; Kneller and Branney, 1995) with high sediment load fallout (Arnott and Hand, 1989; Talling et al., 2012)	Channel axis, lobe axis and lobe off-axis
Structured sandstone (F2)	fs to vfs	Beds 0.1–1 m	Planar, current-ripple, low-angle climbing-ripple or wavy laminations; normal grading; bed bases are sharp or loaded; bed tops are sharp and flat or undulating	Deposited by low-density turbidity currents. Planar and current-ripple lamination produced by dilute flows tractionally reworking the bed top (Allen, 1982, 1973; Best and Bridge, 1992). Climbing- ripple lamination forms under bedload transport associated with high sediment load fallout (Hunter, 1977; Jobe et al., 2012)	Lobe off-axis, channel margin, CLTZs
Hybrid beds (F3)	fs to vfs	Beds 0.1–2 m thick	Comprise two divisions. Lower division: well sorted and "clean"; Upper division can be: (1) mudstone- and siltstone-clast rich with a clean matrix; (2) argillaceous, poorly sorted sandstone with swirly and patchy fabric comprising mudstone chips and carbonaceous material.	Deposited from strongly stratified transitional flows (Baas et al., 2011; Kane and Pontén, 2012; Talling, 2013; Kane et al., 2017) or from co-genetic turbidity currents (lower division) and cohesive debris flows (upper divisions) (Haughton et al., 2003, 2009; Hodgson, 2009)	Deposited in lobe axis, lobe off-axis and lobe fringe environments
Debrites (F4)	fs to vfs	Beds 0.2–3 m	Poorly sorted; mud-rich; matrix supported with variable amounts of mudclasts and carbonaceous material	*En masse* deposition from debris flows (Middleton and Hampton, 1973)	Not indicative of any environment
Contorted and chaotic deposits (F5)	vfs to silt	Beds cms – 2 cm thick, packages up to 5 m thick, extending laterally up to 5 m	Sandstone and siltstone, coherently folded to highly disaggregated	Deposited by remobilization processes to form slides and slumps	Not characteristics of any specific environment
Interbedded sandstone and siltstone packages (F6)	vfs to silt	Beds 0.5–6 cm thick, packages 0.2–5 m thick. Beds tabular or show thickness change with ripple geometries	Sandstone beds show planar, wavy, current-ripple lamination; siltstones are structureless to planar laminated; normal grading; sharp bed bases; undulating tops due to preservation of ripple crests	Deposits of low-density flows. Ripple lamination form beneath dilute turbulent flows via reworking of the bed under moderate sediment load fallout, whereas climbing-ripple lamination forms under high sediment load fallout (Allen, 1971)	Lobe fringe environments
Siltstone (F7)	fine to coarse silt	Beds 0.01–0.15 m	Structureless, planar-laminated or current-ripple-laminated (where sandy); some bioturbation	Deposited by dilute turbidity currents. Planar lamination is a product of traction (Best and Bridge, 1992). Structureless beds are formed by direct suspension fallout (Bouma, 1962)	Lobe distal fringe environments
Claystone (F8)	clay	mm to 10's of meters	Commonly silty; concretions associated with distinctive horizons	Background hemipelagic deposition with occasional suspension fall-out from distal dilute turbidity currents	Hemipelagic background deposits
Discordant layers of sandstone (F9)	fs to vfs	Beds 0.01–2 m thick	Clean to argillaceous very fine to fine-grained sandstone, cross-cutting stratigraphy. Common plumose patterns on fracture surfaces, parallel ridges, mudstone clast-rich surfaces and planar surfaces.	Occurs when: (i) pore pressure in the parent sand body is higher than that within the mud-prone host strata, and (ii) the parent body is composed of clean, fine to very fine unconsolidated sand that is most susceptible to fluidization and grain transport (Richardson, 1971; Jolly and Lonergan, 2002; Cobain et al., 2017). These can be horizontal (sills) or (sub-) vertical (dike) injections.	Injectite

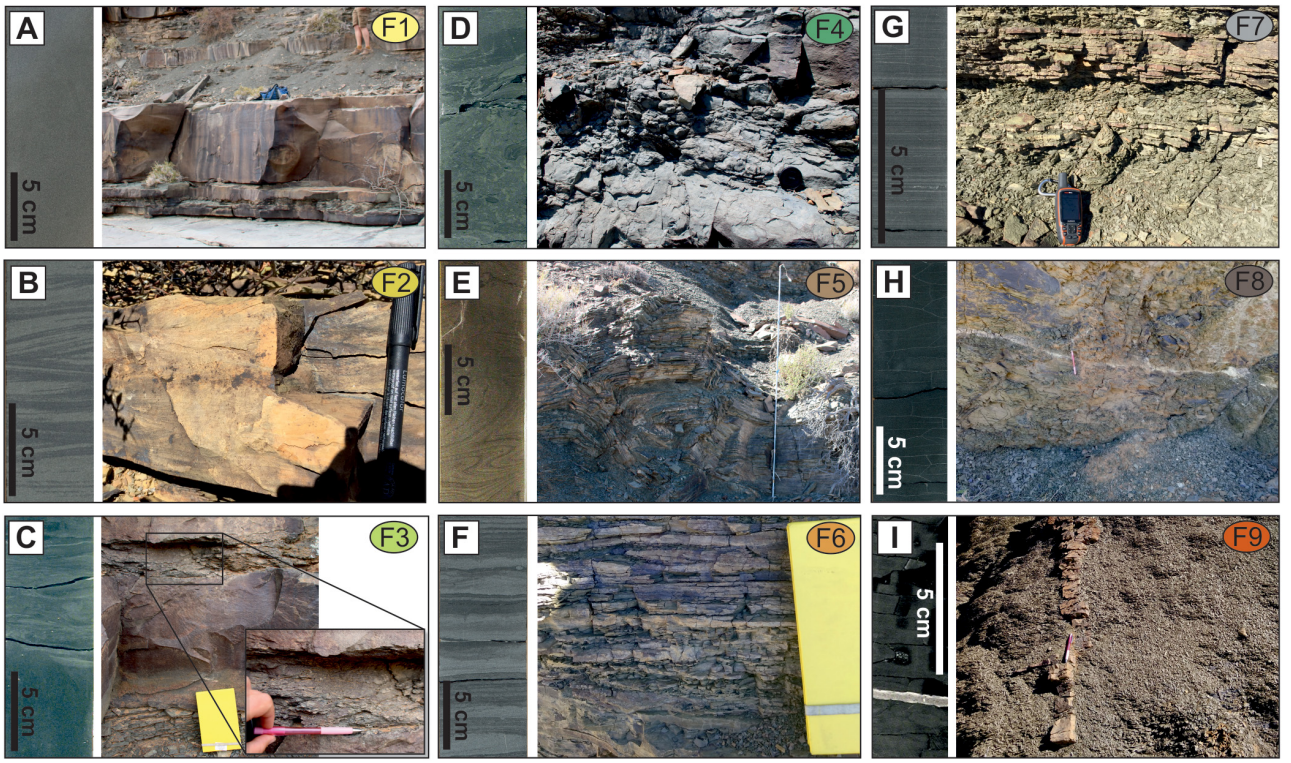

FIGURE 3 | Representative outcrop and core photographs of observed sedimentary facies. **(A)** Structureless sandstone (F1). Bag for scale (~50 cm). **(B)** Structured sandstone (F2). **(C)** Hybrid bed (F3) with lower clean division and upper mudclast-rich division. **(D)** Debrite (F4). **(E)** Deformed strata (F5). **(F)** Thinly interbedded sandstone and siltstone (F6). **(G)** Thin-bedded siltstone and mudstone (F7). **(H)** Mudstone (F8), note the tuff layer in the center of the mudstone package in the outcrop photograph. **(I)** Discordant sandstone (F9) interpreted as injectite, pen for scale (10 cm).

of climbing ripple laminated beds indicative of high-sediment load fallout due to an abrupt loss of flow confinement (Jobe et al., 2012). Typically, successions fine and thin upward due to decreasing overspill during levee construction (Beaubouef, 2004; Kane et al., 2007). In the Karoo Basin, levees are silt-rich and have been mapped for up to 10 km away from their genetically related channel and thin downdip as the channel approaches the channel-lobe transition zone (e.g., Morris et al., 2014, 2016).

Channel-Lobe Transition Zones

Channel-lobe transition zones (CLTZs) can form in relatively unconfined areas dominated by sediment bypass that separate well-defined channels up-dip from well-defined lobes down-dip (Mutti and Normark, 1987, 1991; Wynn et al., 2002; Brooks et al., 2018), and commonly coincide with abrupt changes in gradient. CLTZs are characterized by relatively thin and discontinuous structureless and structured sandstones dominated by climbing-ripple lamination. Abundant scours can also be present due to flows that underwent hydraulic jumps triggered by the changes in flow velocity and/or density resulting from abrupt changes in gradient and degree of confinement (Komar, 1971; Mutti and Normark, 1987, 1991; García and Parker, 1993; Ito, 2008; Macdonald et al., 2011; Hofstra et al., 2015), which commonly are mantled by mudclast conglomerates.

Lobes

To retain consistency with previous literature, the term 'fan' is retained as a lithostratigraphic term that encompasses a linked system of sandstone and siltstone channel-fills and lobe deposits. Collectively, the lobes of a fan are regarded as a lobe complex (Prélat et al., 2009) (**Figure 4**) or lobe complex set (Prélat and Hodgson, 2013). Lobe complexes are made up of different lobes, which in turn are composed of lobe elements, with beds being the smallest scale and fundamental building block in a distributive system (Prélat et al., 2009). Lobes are subdivided into four sub-environments: lobe axis, lobe off-axis, lobe fringe (lateral and frontal) and distal lobe fringe (**Figure 4**), based on facies, sand content and degree of bed amalgamation (Prélat et al., 2009; Prélat and Hodgson, 2013; Kane et al., 2017). Lobe axis deposits comprise thick-bedded, amalgamated structureless sandstone, deposited by high-energy turbidity currents with high rates of deposition (Prélat et al., 2009). Lobe off-axis deposits comprise medium-bedded, structured sandstones with tractional structures, suggesting lower rates of deposition from comparatively lower energy currents (Prélat et al., 2009). Lateral lobe fringe deposits comprise thin-bedded and very fine-grained normally graded and rippled sandstones, deposited from dilute turbidity currents (Prélat et al., 2009; Spychala et al., 2017b). Frontal lobe fringe deposits are characterized by abrupt lateral changes in thickness and facies characterized by

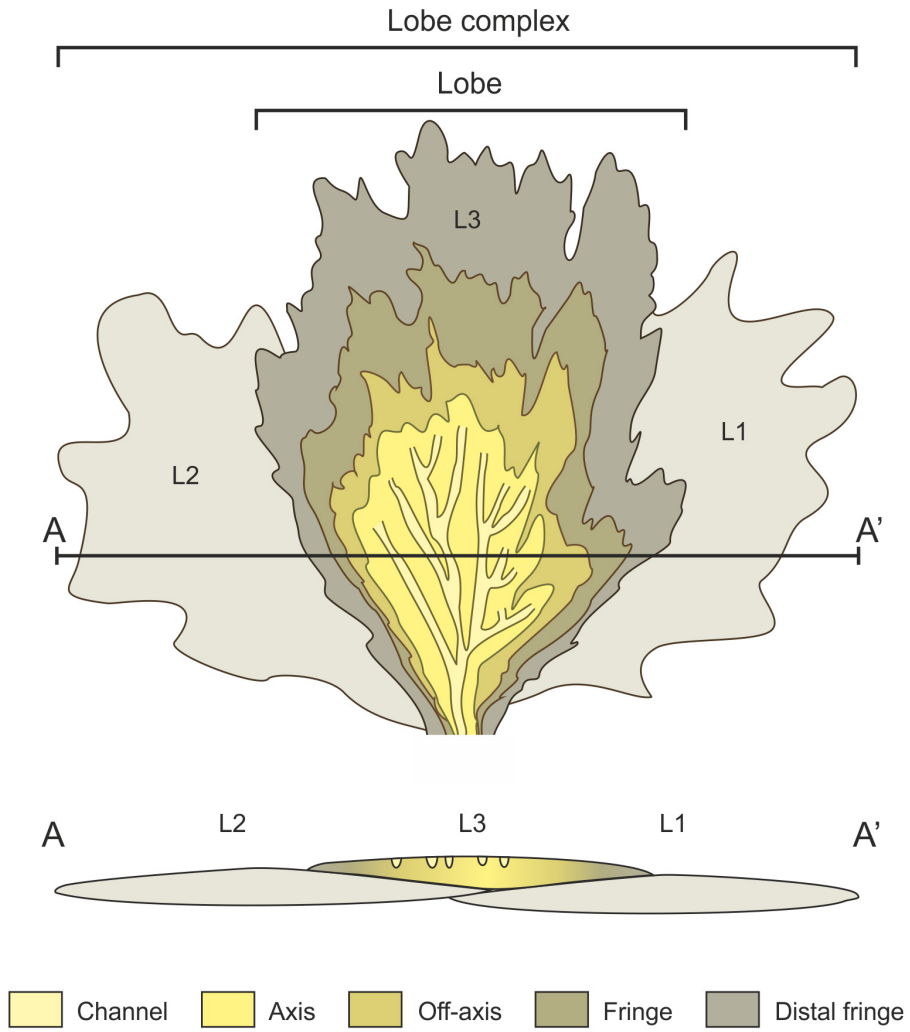

FIGURE 4 | Cartoon indicating the various sub-environments in a lobe, and the stacking of lobes to form a lobe complex.

lenticular sand-rich units that comprise medium- to thin-bedded sandstones and hybrid beds, which pass laterally to thin-bedded sandstone and siltstone units deposited from dilute currents. In planform, these lateral changes form a finger-like geometry (Groenenberg et al., 2010; Spychala et al., 2017b). Hybrid beds in lobe fringe settings are interpreted as deposits from turbidity currents that underwent flow transformation to low yield strength cohesive flows through entrainment of cohesive fine grained substrate and mudclasts (Haughton et al., 2009; Hodgson, 2009; Kane et al., 2017). Distal lobe fringe deposits comprise laterally extensive tapering thin-bedded siltstones.

FAN 3 ARCHITECTURE

The Fan 3 isopach map and regional paleocurrent patterns (from outcrop and FMI measurements from core), indicate a southwestern sediment entry point (Hodgson et al., 2006; Luthi et al., 2006) (**Figure 5**). A northward change in dominant paleocurrent direction from E to NE and NW directed flows, has also been previously documented stratigraphically in wells NB4 and NB3 (Luthi et al., 2006) (**Figure 5**).

In the proximal areas, the cores and outcrop sections demonstrate that the base of Fan 3 comprises a coarsening- and thickening-upward package of siltstone and very fine-grained sandstone, and the top comprises a thinning- and fining- upward succession (Hodgson et al., 2006). In the Gemsbok River valley, Fan 3 comprises six sandstone-rich lobes, which are separated by thin siltstone-prone units (**Figure 6**) (Prélat et al., 2009), interpreted as the distal fringes of other lobes (Prélat and Hodgson, 2013). The lobe stacking patterns within Fan 3 reveal an overall progradational–aggradational–retrogradational trend (Hodgson et al., 2006), with evidence of compensational stacking patterns between lobes (Prélat et al., 2009). The individual lobes have a maximum thickness of 10 m (Prélat et al., 2009), although thicker sandstone units occur where lobes are amalgamated (Hodgson et al., 2006).

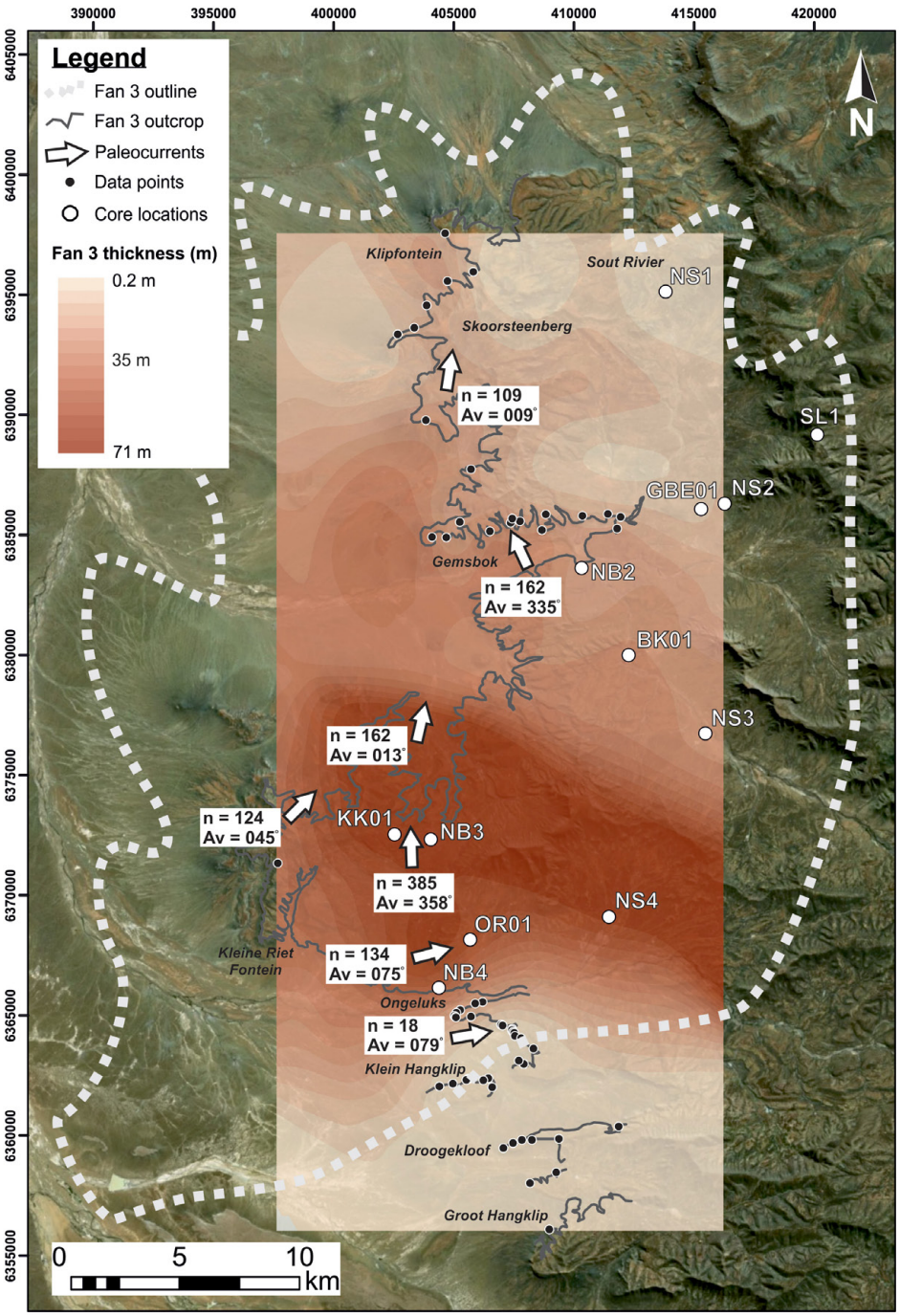

FIGURE 5 | Isopach thickness map of Fan 3 constrained from integration of core and outcrop data taken from this and previous studies (Hodgson et al., 2006; Prélat et al., 2009; Spychala et al., 2017b). Note the rapid thinning in the southern area compared to the rest of the isopach map. Average paleocurrent measurements are also indicated by the white arrows.

The Fan 3 lobe complex has a maximum thickness of 71 m in well NB3 and gradually thins northward over 35 km before reaching the frontal pinchout ~8 km north of NS1 (**Figure 5**). Fan 3 gradually thins laterally in Gemsbok valley, while in the south Fan 3 thins abruptly from OR1 toward Klein Hangklip (**Figure 5**).

FAN 4 ARCHITECTURE

Fan 4 comprises two sandstone prone intervals (lower and upper Fan 4) with different thickness and paleocurrent patterns, which are separated by a thin-bedded siltstone package (Wickens and Bouma, 2000; Hodgson et al., 2006; Spychala et al., 2017b).

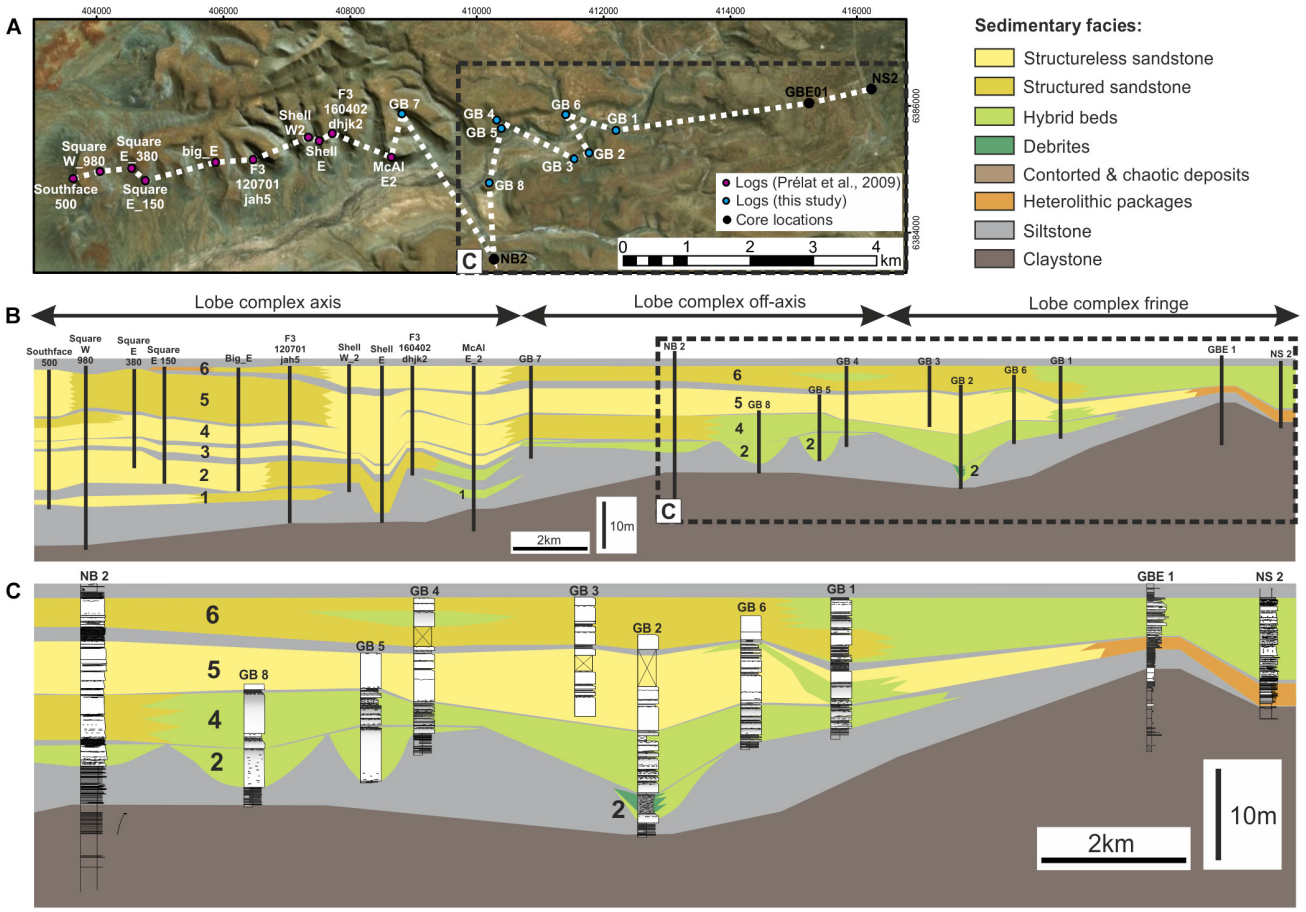

FIGURE 6 | (A) Map of Gemsbok valley showing the log and core locations included in this correlation. **(B)** Lateral pinchout correlation of Fan 3 in Gemsbok valley color coded by the dominant sedimentary facies at any one location. Note the amalgamation of lobes 4 and 5 in the lobe complex axis. **(C)** Zoom in of the easternmost part of the lateral pinchout of Fan 3.

Lower Fan 4 comprises one sandstone-prone lobe complex, whereas upper Fan 4 comprises two sandstone-prone lobe complexes, (Spychala et al., 2017b), with the thin-bedded heterolithic package interpreted as the distal fringe of another lobe complex, meaning that Fan 4 is a lobe complex set (Prélat and Hodgson, 2013). Paleoflow is toward the north and northeast but around Skoorsteenberg (**Figure 2**), a disperse NE to SE paleoflow pattern was recorded in upper Fan 4, interpreted to represent two distinct sediment entry points with deposition from two coeval systems (Dudley et al., 2000; Wickens and Bouma, 2000; Hodgson et al., 2006; Spychala et al., 2017b). Unlike lower Fan 4, there is a lack of clear facies distribution trends in upper Fan 4 pointing to a complicated interaction of depositional systems sourced from the south and west (Spychala et al., 2017b).

Both lower and upper Fan 4 pinch out toward the north with the lobes in lower Fan 4 showing distinct pinch and swell geometries dominated by structureless sandstone and hybrid beds (Spychala et al., 2017b). Lower and upper Fan 4 also thin abruptly southward, but at a lower rate than Fan 3.

LATERAL PINCHOUT OF FAN 3

Fan 3 thins and shows marked facies changes from cores NB2 to NS2 in Gemsbok valley, and is interpreted as the lateral pinchout of the Fan 3 lobe complex (**Figures 5**, **6**) (Hodgson et al., 2006; Prélat et al., 2009). The lobe complex axis (e.g., log Shell E, **Figure 6B**) is dominated by thick-bedded structureless, ripple cross-laminated, and planar laminated very fine- to fine-grained sandstones, with local amalgamation of lobes (**Figure 6**). Turbidite sandstone content decreases from ∼80 to 10% eastward toward the lobe complex fringe at NS2, with a concomitant increase in hybrid beds from ∼8 to 70% (**Figure 7A**). Debrites are rare, and the percentage of heterolithic thin beds in the lobe complex increases from ∼20% at the axis to 50% at the fringe (**Figure 7A**). The lobe complex thins at a rate of 2 m/km. Given that multiple lobes pinchout in this area of marked thinning, we interpret the presence of an approximately west-facing intrabasinal slope. If all the thinning is attributed to this slope then the gradient was ∼0.1° (**Figure 7A**). The six sandstone-rich lobes in the Fan 3 lobe complex show different patterns of facies changes toward the lateral pinchout (**Figure 6**).

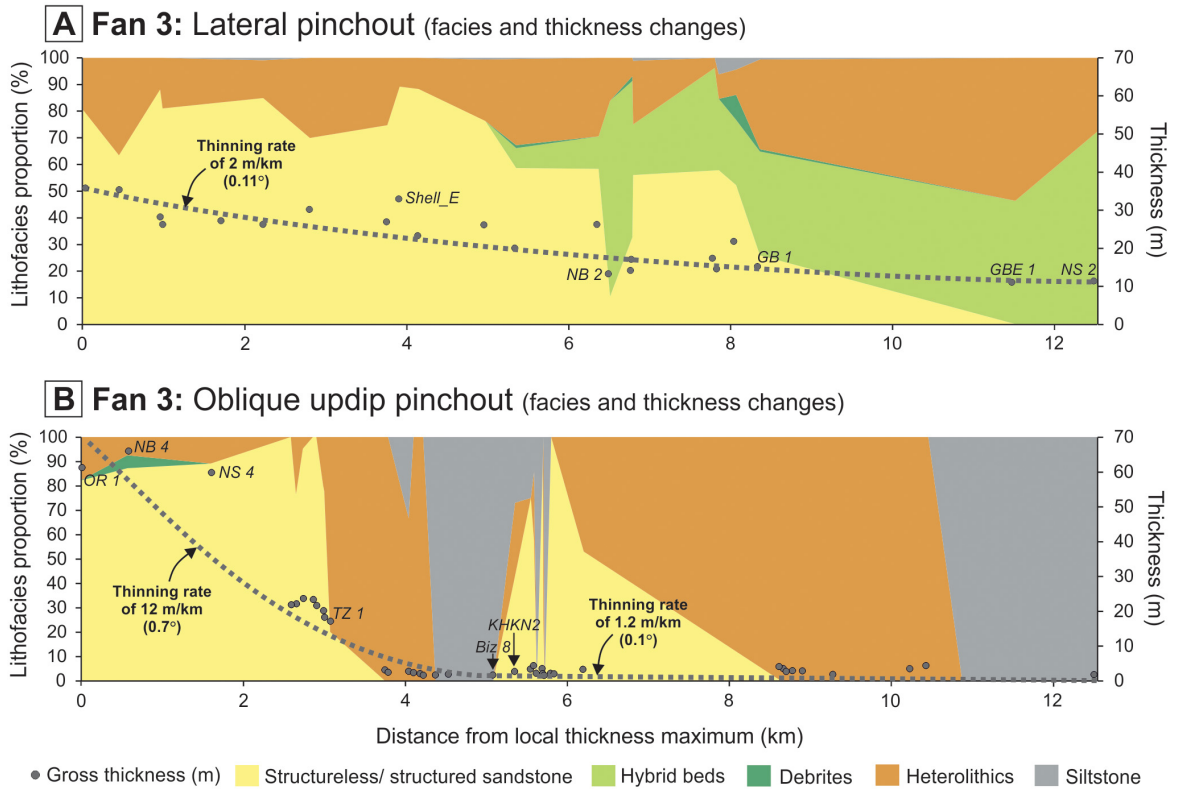

FIGURE 7 | (A) Facies and thickness changes of the lateral pinchout of Fan 3 (location shown in **Figure 2**) showing a gradual decrease in thickness toward the lateral pinchout of Fan 3 and a decrease in sandstone content while the percentage of hybrid beds increases. **(B)** Facies and thickness changes of the oblique up-dip pinchout of Fan 3 (location shown in **Figure 2**) showing an abrupt decrease in Fan 3 thickness and sandstone content. Percentage sandstone increases again at 6 km from the local maximum fan thickness. Note that the thickness and facies proportions were calculated only over the correlative stratigraphic interval and the trendlines are only indicative of the overall trend and not mathematically derived.

The lateral lobe fringes of lobes 1 to 4 are dominated by hybrid beds and their eastern pinchout occurs further west than in the other lobes. There is an eastward increase in lenticular sandstone bodies at the base of Fan 3, which are interpreted as lobe fingers within lobes 1 and 2 (**Figures 6B,C**) (Prélat et al., 2009; Groenenberg et al., 2010). Lobe fingers are dominated by mudclast-rich, very fine- to fine-grained sandstone at their center and thin-bedded hybrid beds or debrites toward the margins, and do not show any evidence of erosion on their basal surface. Typically, the fingers are 200–300 m in strike width, which is consistent with previous studies that document fingers in the distal Fan 3 (Prélat et al., 2009; Groenenberg et al., 2010) and Fan 4 (Spychala et al., 2017b). Spychala et al. (2017b) were able to constrain a dip length of fingers in Fan 4 of approximately 1.5 to 2 km. Injectites are not observed along the lateral pinchout of Fan 3. Eastward, Fan 3 passes into the subcrop, but two cores, from wells GBE1 and NS2, are available 4 km to the east of log GB1, which show that lobes 5 and 6 are still present in these locations (**Figures 6B,C**). They are dominated by heterolithic deposits and hybrid beds, respectively, but the ultimate eastern pinchout of these lobes is unknown.

OBLIQUE UP-DIP PINCHOUT

Fan 3

The paleogeographic configuration indicates that the southern termination of Fan 3 is an oblique up-dip pinchout. In the proximal part at NB4, Fan 3 is 60 m thick (**Figures 8**, **9A,B**) and composed of thick- to medium-bedded structureless and ripple and climbing-ripple dominated sandstone (**Figure 8**). At Ongeluks River, Fan 3 comprises low aspect-ratio channel-fills dominated by amalgamated structureless sandstones that incise sandstone-prone lobe deposits (Sullivan et al., 2000; Hofstra et al., 2017, 2015). West of Ongeluks River at Kleine Riet Fontein (**Figure 2**) Fan 3 is characterized by numerous meter-scale scour features interpreted as a base-of-slope setting with channel-lobe transition zone deposits locally preserved (Luthi et al., 2006; Jobe et al., 2012; Hofstra et al., 2015). Toward the south-east, at log OS2, Fan 3 is 23 m thick and composed of thick to medium-bedded sandstone dominated by climbing-ripple lamination with rare structureless sandstone (**Figure 8**). Less than 4 km to the south-east at log Biz 1, Fan 3 is 1.8 m thick and comprises thin-bedded structured sandstone and heterolithic deposits (**Figures 8**, **9B,C**). Bed terminations indicate

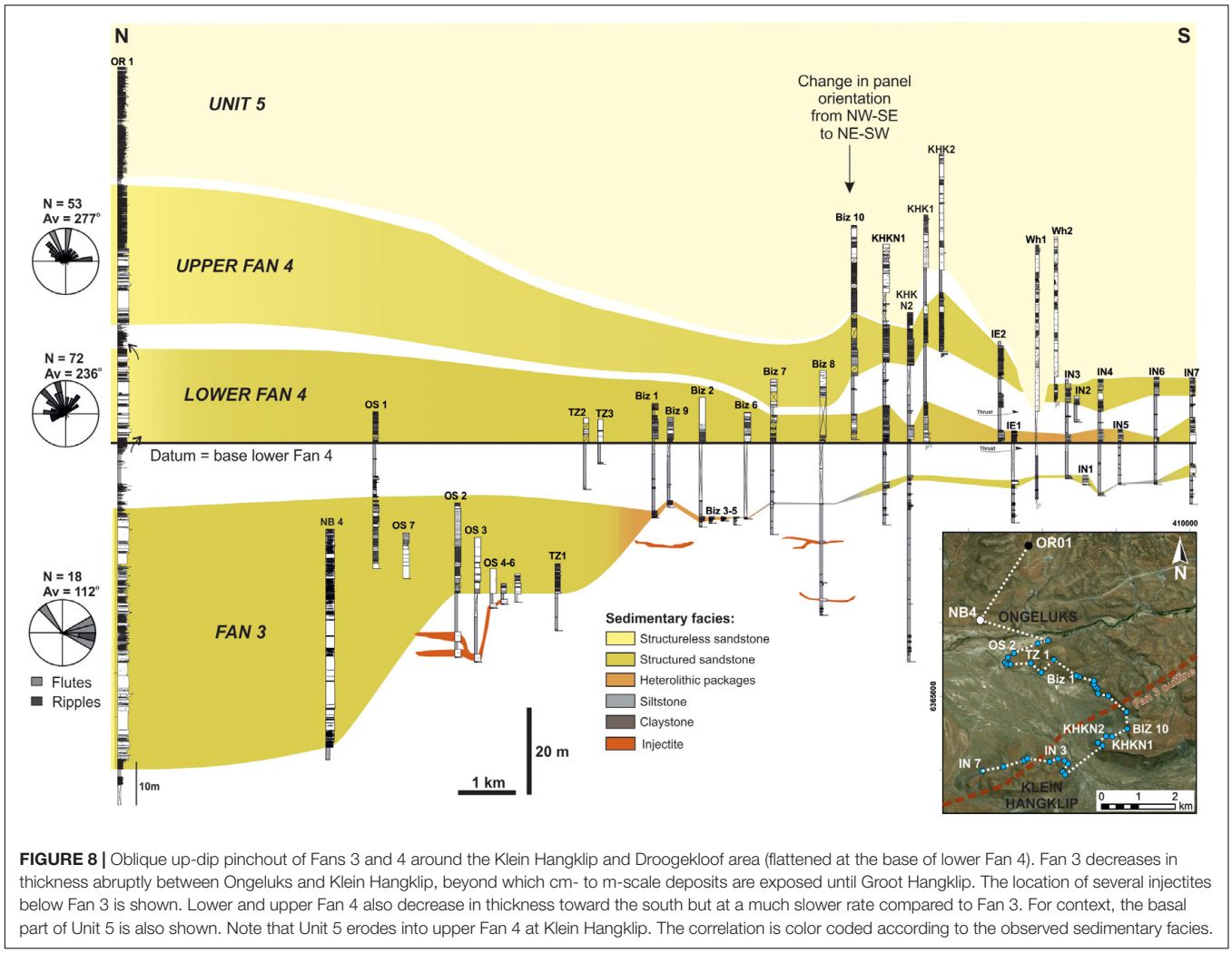

FIGURE 8 | Oblique up-dip pinchout of Fans 3 and 4 around the Klein Hangklip and Droogekloof area (flattened at the base of lower Fan 4). Fan 3 decreases in thickness abruptly between Ongeluks and Klein Hangklip, beyond which cm- to m-scale deposits are exposed until Groot Hangklip. The location of several injectites below Fan 3 is shown. Lower and upper Fan 4 also decrease in thickness toward the south but at a much slower rate compared to Fan 3. For context, the basal part of Unit 5 is also shown. Note that Unit 5 erodes into upper Fan 4 at Klein Hangklip. The correlation is color coded according to the observed sedimentary facies.

stratigraphy is lost from the base of Fan 3, and is equivalent to a thinning rate of 12 m/km, suggesting onlap onto a northwest facing slope of approx. 0.7° (**Figure 7B**). Southward from log Biz 1, the thinning rate decreases to 1.2 m/km, suggesting onlap onto a slope of approx. 0.1° (**Figure 7B**). In planform, this pinchout geometry is not a smooth termination, rather there is localized thinning and thickening and repeated presence of a thin structured sandstone (**Figure 8**). This variation in thickness is also reflected in the sandstone content of Fan 3, which decreases from 80 to 100% at OR1, NS4 and NB4 where Fan 3 is thickest, to 0% around logs TZ1 to Biz 8 (**Figure 7B**). Here, the succession is dominated by interbedded thin (<0.5 m) siltstone packages, with subordinate sandstone beds, before the sandstone content increases again at KHKN1 and KHKN2 (**Figures 7B**, **8**). At the southern pinchout in the Droogekloof area, Fan 3 is dominated by heterolithic deposits and siltstone (**Figure 8**). No hybrid beds are observed at the oblique up-dip pinchout of Fan 3.

Individual lobes are difficult to distinguish in the oblique up-dip pinchout due to amalgamation and erosion by the sand-rich distributary channel-fills in the thickest part of the Fan 3 lobe complex. Near the area of most abrupt thinning a number of clastic injectites are observed below Fan 3, interpreted to originate from Fan 3 and follow the pinchout (**Figures 8**, **9**) (Cobain et al., 2017).

Fan 4

At OR1, lower Fan 4 is 25 m thick and dominated by structureless and structured sandstones with a basal thickening-upward, and an upper thinning-upward package of heterolithics marking the top and base of lower Fan 4 (**Figure 8**). Lower and upper Fan 4 are separated by a 6 m thick unit of heterolithic deposits (**Figure 8**). Upper Fan 4 is 34 m thick at OR1 with the lower 15 m composed of structureless and structured sandstones, and localized hybrid beds, while the upper 20 m is composed of ripple-dominated thin-bedded sandstones (**Figure 8**). Southeast toward Klein Hangklip, lower Fan 4 gradually thins to 3 m thick [thinning rate of 3.7 m/km (**Figure 10**)] and comprises fining- and thinning-upward packages of thin- to medium-bedded climbing ripple laminated sandstones with paleocurrents indicating a northwesterly flow direction (**Figures 11A,B,D**).

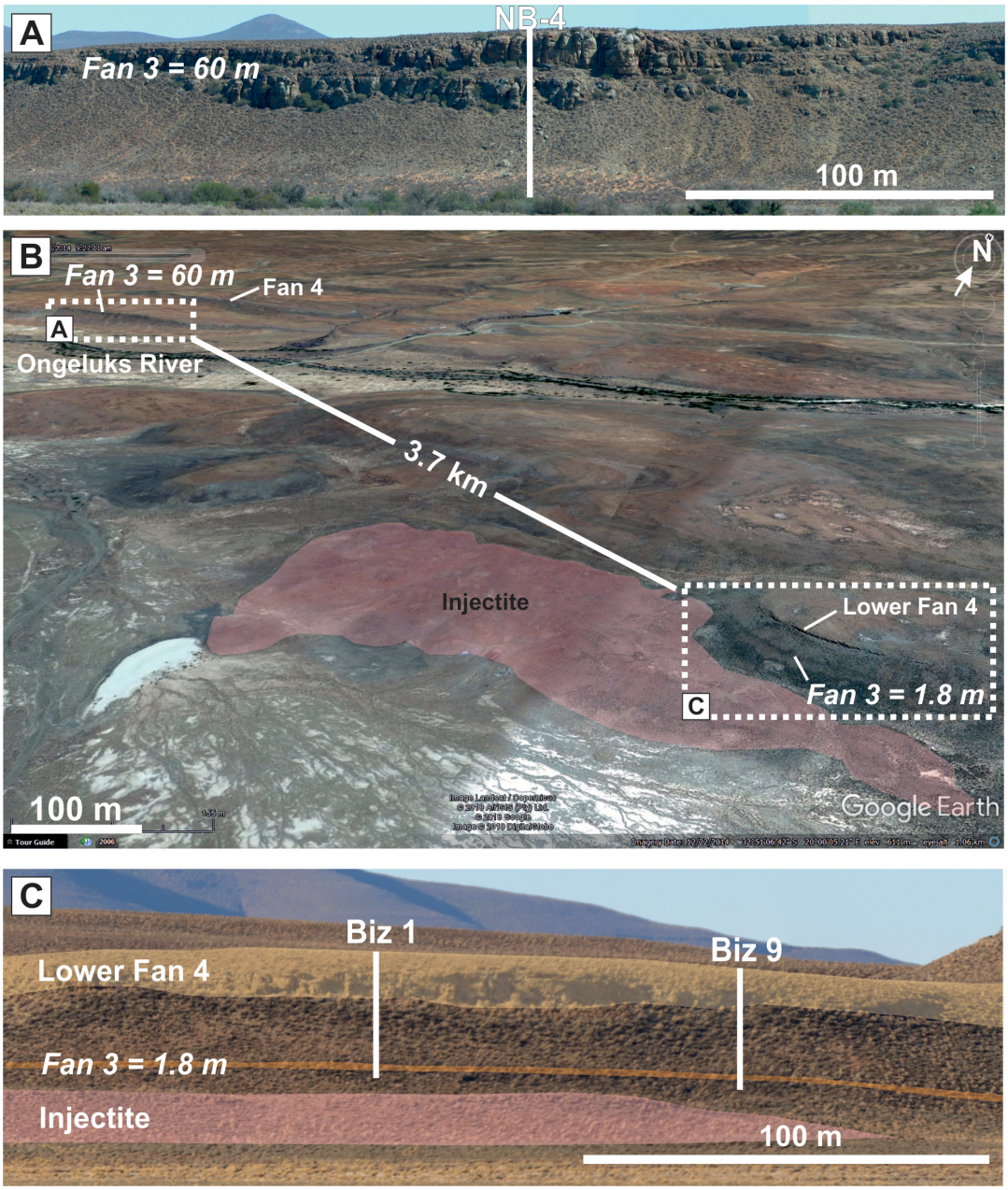

FIGURE 9 | Photos and Google Earth view of the oblique up-dip pinchout of Fan 3. **(A)** Photo of the Fan 3 outcrop at Ongeluks River where it is 60 m thick. **(B)** Google Earth map of the oblique up-dip pinchout area indicating the location of **A** and **C** as well as the location of the injectite complex. **(C)** Photo of Fan 3 and lower Fan 4 showing the rapid thinning of Fan 3 over 3.7 km to the SE of Ongeluks River.

Multiple meters-wide scours, with erosion of 10's cms, are mantled with mudclasts within and toward the top of lower Fan 4 (**Figures 11F,G**). Generally, upper Fan 4 is sandier than lower Fan 4, with paleocurrents indicating northwesterly flow (**Figures 11A,B,D,E**). Upper Fan 4 thins to 8 m at Klein Hangklip [thinning rate of 4.3 m/km (**Figure 10**) where it is dominated by medium bedded, climbing ripple dominated sandstone with some scours (**Figures 11A,B,E**). Injectites are not observed.

DISCUSSION

Comparison Between Up-Dip, Lateral and Frontal Pinchouts

The difference in calculated slope gradients between the oblique up-dip and basinward lateral pinchouts indicate that the eastern margin of Fan 3 was less confined by seabed topography compared to the up-dip southern margin (**Figure 12A**). The steeper seabed topography in the up-dip area meant there

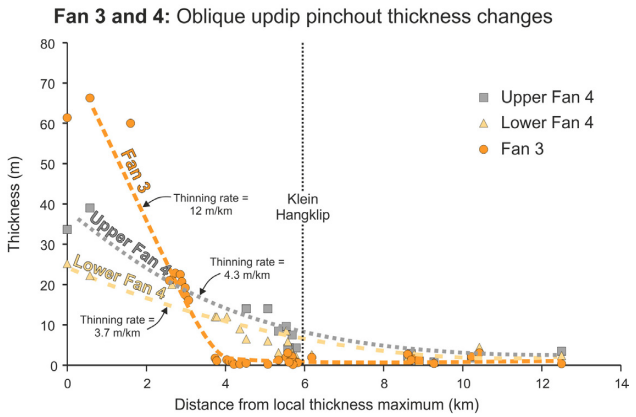

FIGURE 10 | Thickness changes of Fan 3, lower Fan 4 and upper Fan 4 at the oblique up-dip pinchout derived from the correlative stratigraphic interval, showing that the decrease in Fan 3 thickness is much more abrupt compared to lower and upper Fan 4. Note that the trendlines are only indicative of the overall trend and not mathematically derived.

was limited accommodation. This is reflected in channels cutting proximal lobes (Hofstra et al., 2017), widespread scours mantled with mudclasts indicating sediment bypass (Sullivan et al., 2000; Hofstra et al., 2015; Stevenson et al., 2015), and the development of aggradationally stacked and amalgamated lobes (**Figure 12D**). Abrupt sand-rich up-dip pinchouts can be characterized by the presence of clastic injectites. The compaction drive promoted by the abrupt pinchout architecture, the sealing mudstone both below and above sharp Fan 3 boundaries, and the clean, proximal sandstone beds, and the resulting overpressured sandbodies is interpreted to encourage sandstone injection (Cobain et al., 2017). In contrast, the tapered pinchouts, the heterolithic base and tops of Fan 3, and the less clean sandstones at the lateral and frontal pinchouts inhibits clastic injection processes (Cobain et al., 2017).

A variety of different facies transitions occur in individual lobes toward the lateral pinchout of the Fan 3 lobe complex. Hybrid bed-dominated lobe fingers represent the frontal pinchouts of lobes 1 and 2 (Prélat et al., 2009) (**Figure 12C**). The eastern pinchouts of lobes 3 to 5 are interpreted as lateral (lobes 3 and 5) and frontal (lobe 4) lobe fringes following the criteria of Spychala et al. (2017b), whereas lobe 6 has a highly asymmetric facies distribution in 2D. The vertical stacking pattern of the lobes suggests aggradational stacking of the lower lobes 1 and 2, which may have largely healed pre-existing topography, resulting in lobes 3 to 6 being less confined and able to stack compensationally instead (Prélat and Hodgson, 2013; Spychala et al., 2017b). Therefore, in a 1D section, both frontal and lateral fringes of different lobes are intersected at the lateral fringe of the Fan 3 lobe complex (**Figure 12C**). This illustrates that taking a hierarchical approach to the analysis of deep-water stratigraphy is needed to improve the assessment of basin-floor pinchouts.

In comparison, the frontal pinchout of Fan 3 has not been reported to have been affected by seabed topography and individual lobes are distinguishable (Kane et al., 2017) (**Figures 2**, **12B**). Distal lobe fingers exhibit greater abundance of hybrid beds toward the fontal pinchout (Spychala et al., 2017b) (**Figure 12B**). The flows depositing the hybrid bed- and debrite-dominated lobe fingers at the frontal pinchouts of lobes have been interpreted as cohesive and elongate, which loaded onto the substrate to form subtle seabed topography that subsequent flows followed (Groenenberg et al., 2010). Hybrid beds in frontal lobes of Fan 3 are interpreted to be the result of erosion of cohesive substrate farther up-dip that transformed a turbidity current to a low yield strength cohesive flow resulting in a catastrophic loss of turbulence and flow collapse (Kane et al., 2017).

Lobe stacking patterns at the different pinchout margins of a lobe complex depend on both autogenic (e.g., channel avulsion and compensational stacking) and allogenic factors (e.g., tectonic control on basin physiography, sediment supply), which can impact the sediment supply to the deep water (Prélat et al., 2009). In unconfined settings, lobes are more likely to stack compensationally so different parts of lobes are able to stack in a 1D section, as seen at the lateral pinchout of Fan 3 (Prélat et al., 2009; Spychala et al., 2017b). In a confined setting, lobes are forced to stack more aggradationally or longitudinally rather than compensationally (Marini et al., 2016; Spychala et al., 2017a,b), as seen in the oblique up-dip pinchout of Fan 3.

Comparison of Fan 3 and Fan 4 Up-Dip Pinchouts

The depositional architecture of the Fan 3 and 4 oblique up-dip pinchouts demonstrate that the style of pinchout can be markedly different even in successive units in the same basin position.

Comparatively steep seabed topography in the up-dip area results in the abrupt thinning of lobe complexes, as observed in Fan 3 (**Figures 8**, **12**, **13**). Beyond the thickest part of Fan 3, a ∼m-thick succession of structured sandstone and heterolithic deposits continues for 2.5 km (in a straight line) (**Figures 8**, **11C**, **12**, **13**). In the absence of timelines, the exact temporal relationship between the deposition of the thicker and thinner part of Fan 3 is unclear. Deposition may have occurred simultaneously if the axial flows depositing the sediment in the thicker part around Ongeluks and Bizansgat were stripped to form overbank deposits. Alternatively, the thick channel-dominated part of Fan 3 was deposited first and in-filled the pre-existing seabed topography, after which the thinner southern part was deposited by smaller volume flows above a lower gradient slope. If flow stripping occurred throughout Fan 3 activity, then the thin part of Fan 3 would be dominated by heterolithic deposits, which would potentially show a fining and thinning upward profile, similar to external levees. While heterolithic facies are present in this area, the presence of medium- to thick-bedded structured sandstones suggest that sand sedimentation mainly occurred after most of the seabed topography was healed.

The change in architecture, thickness decay and sedimento-logical characteristics between Fans 3 and 4 suggests a marked change in depositional environment and basin configuration. The

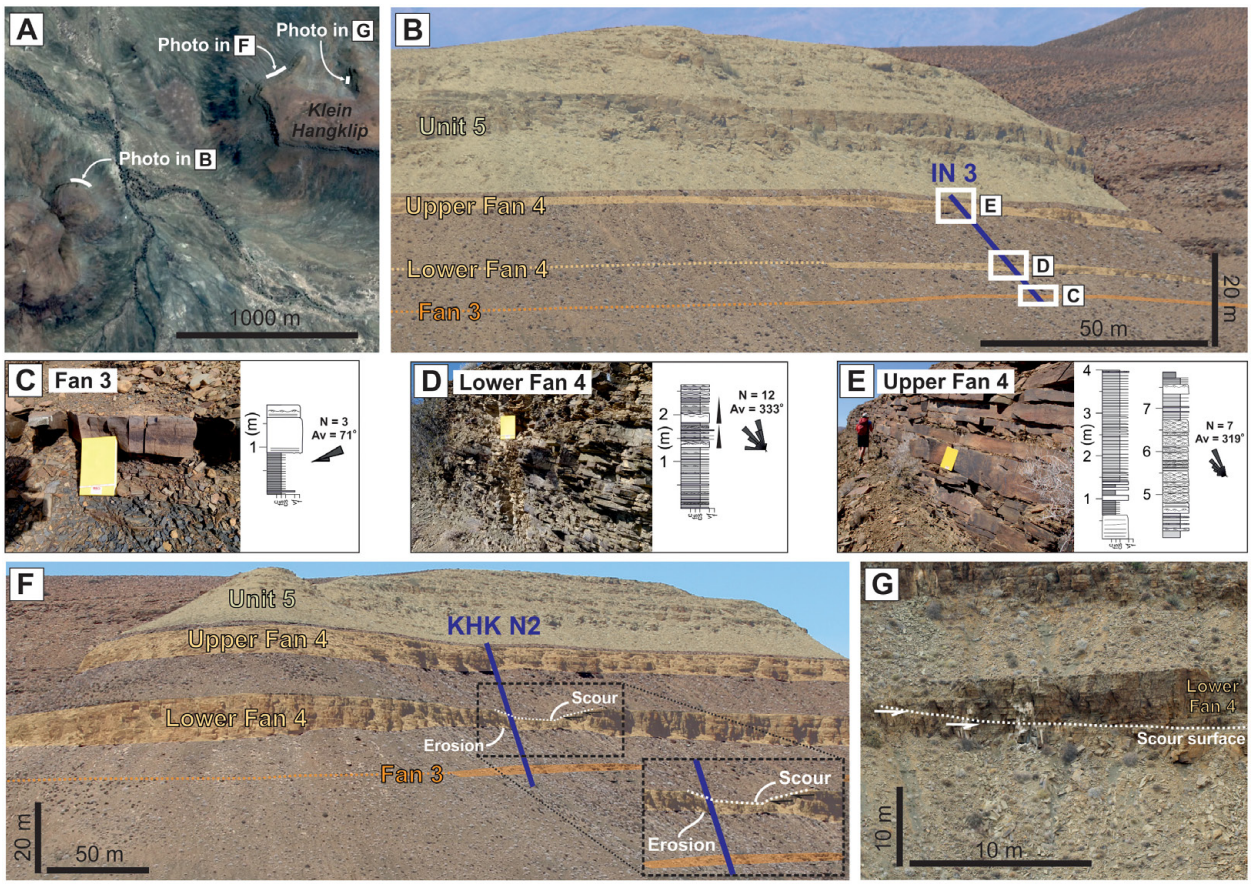

FIGURE 11 | (A) Location map of photo panels. **(B)** View of the western side of Klein Hangklip west showing Fan 3, lower and upper Fan 4. **(C–E)** Photos and sedimentary logs of Fan 3, lower and upper Fan 4 from log IN3 showing their typical appearance in this area. **(F)** View of the eastern side of Klein Hangklip showing Fan 3, lower and upper Fan 4. Location of log KHK N2 is indicated. **(G)** Photo of scour in lower Fan 4, location indicated in **(A)**.

abundance of scours mantled with mudclasts in lower Fan 4 at Klein Hangklip indicates that this area was subject to erosion and sediment bypass, and shares characteristics with CLTZs elsewhere in the basin (Hofstra et al., 2015; Brooks et al., 2018). Farther south at Droogekloof, the thinning and fining upward packages of thin-bedded rippled sandstones are characteristic of external levees (Morris et al., 2014) with the northwesterly paleocurrents indicating flow perpendicular to the main Fan 4 sediment input point (**Figure 11D**). This configuration supports an interpretation of external levees that interfingered with a bypass-dominated CLTZ across strike to form a dip-oriented levee-lobe transition zone, in a more proximal position than Fan 3 (**Figure 13**). Healing of local seabed topography by Fan 3 may have promoted the basinward progradation of Fan 4. In contrast, external levee deposits are not identified in upper Fan 4, and the sandier and thicker-bedded nature together with less widespread evidence for sediment bypass suggests that this area was either (i) not in close proximity to an up-dip CLTZ, or (ii) that the CLTZ was not as well developed as there was no longer a pronounced break-in-slope, leading to proximal lobe deposition close to the upper Fan 4 pinchout (**Figure 13**). Differences in thickness decay and sedimentological characteristics between the up-dip pinchouts of Fans 3 and 4 indicate that the healing of seabed topography and subtle changes in slope gradient lead to markedly different pinchout architecture.

Implications for Stratigraphic Trap Prediction

The documented up-dip, lateral and frontal basin floor fan pinchouts characteristics are all at sub-seismic scale, and are summarized in **Table 2**. The constraints afforded by outcrop studies are vital to better understand risks and uncertainties when assessing basin-floor fan pinchouts as potential stratigraphic traps for hydrocarbon reservoirs. Generally, up-dip pinchouts have a higher sandstone percentages (up to 100%), which decreases abruptly near the pinchout. While the rate of thickness decrease is high, the dominance of structureless and structured sandstone means that permeability and porosity values likely remain high. In the described example from Fan 3, as well as in other studies (Brooks et al., 2018), a thin sandstone or heterolithic package continues up-dip, which can create the potential for up-dip leakage of hydrocarbons. While faulting can easily offset the presence of these thin sandstone and heterolithic

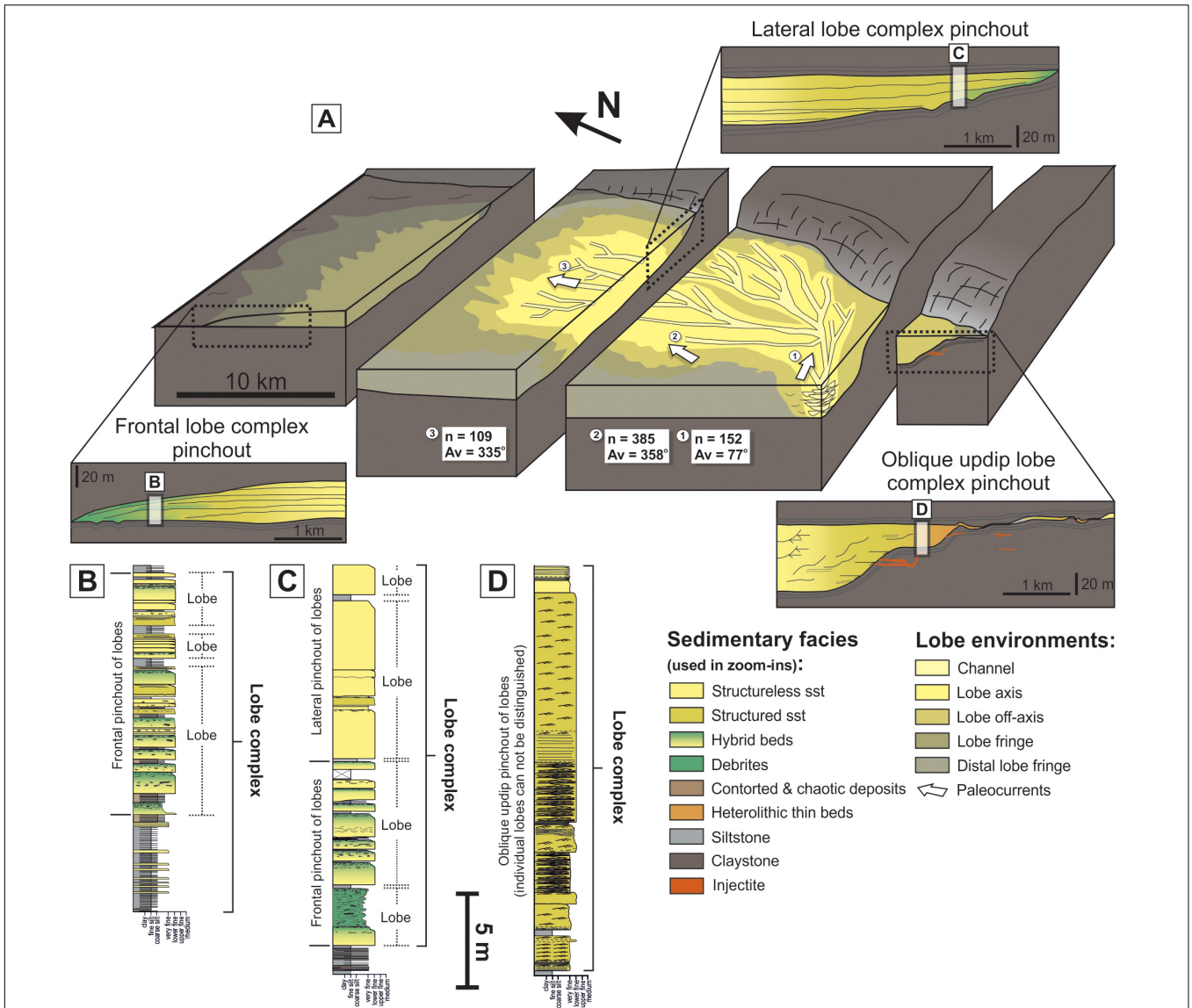

FIGURE 12 | (A) Block diagram of the Fan 3 lobe complex indicating the different lobe environments and decrease in topography on the eastern margin toward the north. The oblique up-dip, lateral and frontal pinchouts of Fan 3 are shown in detail and are color coded by sedimentary facies. **(B)** Example sedimentary log through the frontal pinchout of the Fan 3 lobe complex where frontal pinchouts of individual lobes can be distinguished (adapted from Spychala et al., 2017b). **(C)** Example sedimentary log showing a vertical section through the lateral pinchout of the Fan 3 lobe complex where frontal and lateral lobe pinchouts occur in a 1D section. **(D)** Example sedimentary log showing a vertical section through the oblique up-dip pinchout of the Fan 3 lobe complex. Note that the individual lobes cannot be distinguished.

packages in a combination trap, the presence of injectites at up-dip fan pinchouts may further enhance the potential for up-dip hydrocarbon leakage (Cartwright, 2007; Cobain et al., 2017). At the lobe complex-scale, the presence of bed amalgamation, climbing ripple laminated sandstones, injectites, and the lack of hybrid beds may be used to identify this setting in 1D subsurface datasets. However, as demonstrated in this study, it is possible that the up-dip pinchout style changes across multiple lobe complexes, particularly if seabed topography is gradually healed by the deposition of older lobe complexes. In the case of the up-dip pinchout examples, stratigraphic trapping changed from an oblique and abrupt up-dip pinchout of Fan 3 to the gradual up-dip pinchout of lower Fan 4 with the preservation of the levee-lobe transition zone, to the tapered lateral pinchout of upper Fan 4.

Lateral fan fringe deposits decrease much more gradually in thickness and sandstone content toward the pinchout while sandstone content is still high in the lobe axis (up to 92%). The increase of heterolithics and hybrid beds toward the pinchout means that permeability values are likely to be considerably lower than in structureless and structured sandstone, with higher mud content observed in hybrid beds compared to turbidites (Kane

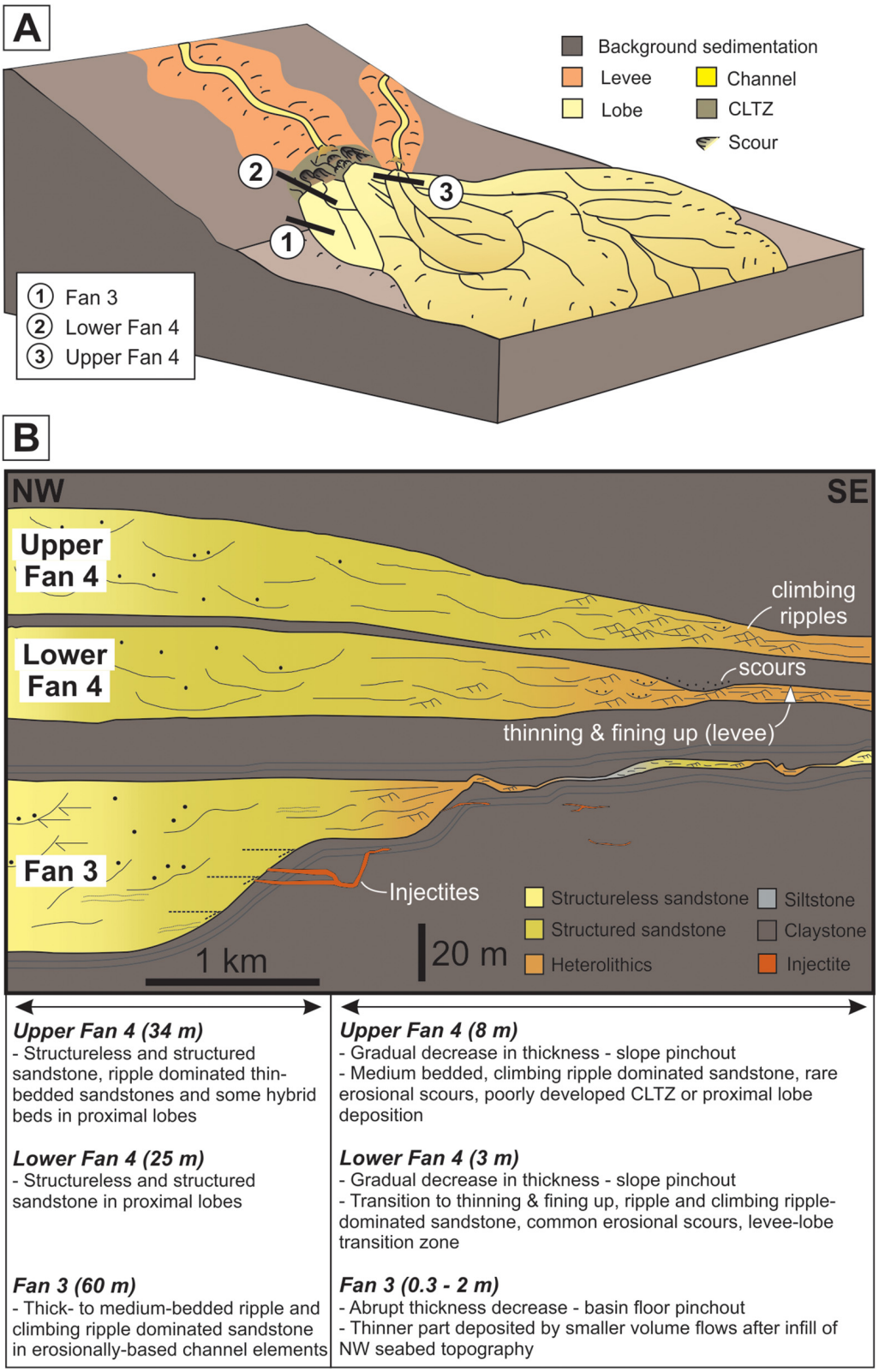

Upper Fan 4 (34 m) - Structureless and structured sandstone, ripple dominated thin-bedded sandstones and some hybrid beds in proximal lobes	***Upper Fan 4 (8 m)*** - Gradual decrease in thickness - slope pinchout - Medium bedded, climbing ripple dominated sandstone, rare erosional scours, poorly developed CLTZ or proximal lobe deposition
Lower Fan 4 (25 m) - Structureless and structured sandstone in proximal lobes	***Lower Fan 4 (3 m)*** - Gradual decrease in thickness - slope pinchout - Transition to thinning & fining up, ripple and climbing ripple-dominated sandstone, common erosional scours, levee-lobe transition zone
Fan 3 (60 m) - Thick- to medium-bedded ripple and climbing ripple dominated sandstone in erosionally-based channel elements	***Fan 3 (0.3 - 2 m)*** - Abrupt thickness decrease - basin floor pinchout - Thinner part deposited by smaller volume flows after infill of NW seabed topography

FIGURE 13 | (A) Schematic summary of a deep-water slope to basin floor transition, indicating the location of the oblique up-dip pinchouts of Fan 3, lower Fan 4 and upper Fan 4. **(B)** Schematic cross-section of the oblique up-dip pinchouts of Fan 3, lower Fan 4 and upper Fan 4, indicating the changes in pinchout architecture between these lobe complex sets. The table includes a summary of the facies and thickness changes toward the pinchout.

TABLE 2 | Characteristics of oblique up-dip, lateral and frontal lobe pinchouts.

	Oblique up-dip pinchout	Lateral pinchout	Frontal pinchout
Pinchout geometries	Abrupt decrease in thickness to meter-scale deposits	Wedge shaped, gradual pinchout	Pinch-and-swell, finger-like geometry with abrupt pinchout
Percentage sandstone	Rapid decrease, 100% in proximal areas	Gradual decrease, 90% in proximal areas	Rapid decrease, 50% in proximal areas
Hybrid beds	Absent	Can be abundant in basal part of lobe complex if frontal pinchouts of lobes are present	Common throughout, both at a lobe and lobe complex scale
Sedimentary structures	Abundant climbing ripples in proximal parts transitioning to rippled and laminated thin-bedded sandstone and siltstone	Current ripple laminations, thick structureless sandstone with mudclasts	Current ripple laminations
Injectites	Present	Absent	Absent
Lobe stacking patterns	Individual lobes are amalgamated and can't be differentiated	Stacking of frontal and lateral lobe fringes	Stacking of frontal lobe fringes only
Reservoir risk	Up-dip leakage	Sandstone quality (waste zone dimension)	Sandstone quality (waste zone dimension)

Details of the frontal pinchout taken from Kane et al. (2017) and Spychala et al. (2017b).

et al., 2017). The combined lateral and frontal lobe pinchout seen in Fan 3 is therefore less likely to leak, due to the permeability associated with the increased volume of hybrid beds. If only the lateral lobe pinchouts are present then hybrid beds are less abundant (Spychala et al., 2017b). Frontal fan fringe deposits are characterized by their abrupt pinch and swell style of pinchout but can still have relatively high sandstone percentage [up to 50% (Spychala et al., 2017b)]. While individual lobe fingers are dominated by hybrid beds, they are still connected to high-quality reservoir sandstone further up-dip.

Individual lobes are about 5 m thick and too thin to image in conventional reflection seismic data, the vertical resolution of which will generally be limited to the lobe complex scale (10's m; Prélat et al., 2010). However, in a 1D dataset, such as core data, it may be possible to use the distinct difference in lobe stacking patterns, sedimentary structures, and facies distribution within individual lobe complexes to better constrain the paleogeographic environment when a hierarchical approach is followed. In the future, compilation of more sub-seismic basin-floor pinchouts, with known paleogeographic contexts, will permit the integration of bed thickness statistics (e.g., Marini et al., 2016) to improve predictions of distance and direction to pinchout points. Nonetheless, stacking patterns can be used to better understand the impact of seabed topography on lobe deposition, which may help to better predict facies distribution vertically as well as laterally within one lobe complex.

CONCLUSION

The up-dip, lateral and frontal pinchouts of lobe complexes in a single basin-fill are distinct in character due to differences in seabed confinement and flow processes that control contrasting facies distributions and stacking patterns of individual lobes. The impact of evolving seabed topography during sedimentation, with infilling and healing of previous topographic lows and break-in-slope, is illustrated at the up-dip pinchouts of Fans 3 and 4, where the infilling of base-of-slope topography by the deposition of Fan 3 resulted in contrasting up-dip pinchout architectures in the overlying Fan 4 system. The change from aggradationally stacking up-dip lobe pinchouts to compensationally stacking lobe pinchouts at the lateral pinchout of the Fan 3 lobe complex also illustrate the impact of spatial differences in seabed topography. Frontal lobe pinchouts can occur both at the frontal and lateral pinchout of a lobe complex, highlighting the importance of identifying hierarchical scale when assessing and modeling these environments as stratigraphic traps for hydrocarbons. The range of pinchout styles onto very subtle (<2°) seabed topography and the variation in stacking patterns of individual lobes within a lobe complex highlight the utility of basin-floor pinchout architecture in improving understanding of basin configurations, and in investigating how subtle seabed topography can influence flow processes. Additionally, the described sub-seismic scale characteristics highlight that outcrop studies are vital when assessing basin-floor pinchouts as potential stratigraphic traps for hydrocarbons.

AUTHOR CONTRIBUTIONS

DH, SF, LH, and AP coordinated the work. All authors discussed the results. LH wrote the manuscript, with support from DH, SF, AP, and DB. DB contributed to data collection and analysis.

FUNDING

This research was funded by Equinor ASA.

ACKNOWLEDGMENTS

The manuscript has benefited from thorough reviews by the reviewers Mattia Marini and Aggie Georgiopoulou. We thank the local farmers of the Tanqua region for permission to undertake field studies on their land, especially De Ville Wickens. We thank Charlotte Allen, Rachel Healy, and David Lee for field assistance. We are grateful for the financial support from Equinor that made this research work possible.

REFERENCES

Allen, J. R. (1971). Mixing at turbidity current heads, and its geological implications. *J. Sediment. Res.* 41, 97–113. doi: 10.1144/gsjgs.129.5.0537

Allen, J. R. L. (1973). A classification of climbing-ripple cross-lamination. *J. Geol. Soc. London* 129, 537–541. doi: 10.1144/gsjgs.129.5.0537

Allen, J. R. L. (1982). *Sedimentary Structures: Their Character and Physical Basis*. Amsterdam: Elsevier.

Amy, L. A., Kneller, B. C., and McCaffrey, W. D. (2007). Facies architecture of the Grès de Peïra Cava, SE France: landward stacking patterns in ponded turbiditic basins. *J. Geol. Soc.* 164, 143–162. doi: 10.1144/0016-76492005-019

Arnott, R., and Hand, B. (1989). Bedforms, primary structures and grain fabric in the presence of suspended sediment rain. *J. Sediment. Res.* 59, 1062–1069. doi: 10.1306/212F90F2-2B24-11D7-8648000102C1865D

Baas, J. H., Best, J. L., and Peakall, J. (2011). Depositional processes, bedform development and hybrid bed formation in rapidly decelerated cohesive (mud-sand) sediment flows. *Sedimentology* 58, 1953–1987. doi: 10.1111/j.1365-3091.2011.01247.x

Bakke, K., Kane, I., Martinsen, O. J., Petersen, S. A., Johansen, T. A., Hustoft, S., et al. (2013). Seismic modeling in the analysis of deep-water sandstone termination styles. *Am. Assoc. Pet. Geol. Bull.* 97, 1395–1419. doi: 10.1306/03041312069

Beaubouef, R. (2004). Deep-water leveed-channel complexes of the Cerro Toro Formation, Upper Cretaceous, southern Chile. *Am. Assoc. Pet. Geol. Bull.* 88, 1471–1500. doi: 10.1306/06210403130

Best, J., and Bridge, J. (1992). The morphology and dynamics of low amplitude bedwaves upon upper stage plane beds and the preservation of planar laminae. *Sedimentology* 39, 737–752. doi: 10.1111/j.1365-3091.1992.tb02150.x

Blewett, S. C., and Phillips, D. (2016). "An overview of cape fold belt geochronology: implications for sediment provenance and the timing of orogenesis," in *Origin and Evolution of the Cape Mountains and Karoo Basin*, eds B. Linol and M. de Wit (Cham: Springer), 45–55.

Bouma, A. H. (1962). *Sedimentology of some Flysch deposits. A Graphic Approach to Facies Interpretation*. Amsterdam: Elsevier.

Bouma, A. H., and Rozman, D. J. (2000). "Characteristics of Fine-Grained Outer Fan Fringe Turbidite Systems," in *Fine-Grained Turbidite Systems*, eds A. H. Bouma and C. G. Stone (Tulsa, OK: AAPG Memoir,), 291–298.

Bouma, A. H., and Wickens, H. D. (1991). Permian passive margin submarine fan complex, Karoo Basin, South-Africa: possible model to Gulf of Mexico. *Gulf Coast. Assoc. Geol. Soc. Trans.* 41, 30–42.

Bouma, A. H., and Wickens, H. D. (1994). "Tanqua Karoo, Ancient analog for fine-grained submarine fans," in *Submarine Fans and Turbidite Systems. Gulf Coast Section SEPM Foundation 15th Annual Research Conference*, eds P. Weimer, A. Bouma, and B. Perkins (Tulsa, OK), 23–34. doi: 10.5724/gcs.94.15.0023

Brooks, H. L., Hodgson, D., Brunt, R. L., Peakall, J., Hofstra, M., and Flint, S. (2018). Deepwater channel-lobe transition zone dynamics — processes and depositional architecture, an example from the Karoo Basin, South Africa. *GSA Bull.* 130, 1723–1746. doi: 10.1130/B31714.1

Carr, M., and Gardner, M. (2000)." Portrait of a basin-floor fan for sandy deepwater systems, Permian lower Brushy Canyon Formation, west Texas," in *Fine-Grained Turbidite Systems: American Association of Petroleum Geologists, Memoir*, Vol. 72, eds A. Bouma and C. Stone (Tulsa, Ok: SEPM Special Publications), 68. pp. 215–232.,

Cartwright, J. (2007). The impact of 3D seismic data on the understanding of compaction, fluid flow and diagenesis in sedimentary basins. *J. Geol. Soc.* 164, 881–893. doi: 10.1144/0016-76492006-143

Cobain, S., Hodgson, D., Peakall, J., and Shiers, M. N. (2017). An integrated model of clastic injectite sand basin floor lobe complexes: implications for stratigraphic trap plays. *Basin Res.* 29, 816–835. doi: 10.1111/bre.12229

De Wit, M. J., and Ransome, I. G. D. (eds) (1992). "Regional inversion tectonics along the southern margin of Gondwana," in *Inversion Tectonics of the Cape Fold Belt, Karoo and Cretaceous Basins of Southern Africa*, (Rotterdam: A.A. Balkema), 15–21.

Deptuck, M., Piper, D., Savoye, B., and Gervais, A. (2008). Dimensions and architecture of late Pleistocene submarine lobes off the northern margin of East Corsica. *Sedimentology* 55, 869–898. doi: 10.1111/j.1365-3091.2007.00926.x

Dudley, P. R. C., Rehmer, D. E., and Bouma, A. H. (2000). "Reservoir scale characteristics of fine-grained sheet sadnstones, Tanqua Karoo Subbasin, South Africa," in *Deep-Water Reservoirs of the World: GCSSEPM Foundation 20th Annual Research Conference*, (Houston, TX: GCSSEPM Foundation), 318–341.

Etienne, S., Mulder, T., Bez, M., Desaubliaux, G., Kwasniewski, A., Parize, O., et al. (2012). Multiple scale characterization of sand-rich distal lobe deposit variability: examples from the Annot Sandstones Formation, Eocene-Oligocene, SE France. *Sediment. Geol.* 27, 1–18. doi: 10.1016/j.sedgeo.2012.05.003

Flint, S., Hodgson, D., Sprague, A. R., Brunt, R., Van der Merwe, W. C., Figueiredo, J., et al. (2011). Depositional architecture and sequence stratigraphy of the Karoo basin floor to shelf edge succession, Laingsburg depocentre, South Africa. *Mar. Pet. Geol.* 28, 658–674. doi: 10.1016/j.marpetgeo.2010.06.008

García, M., and Parker, G. (1993). Experiments on the entrainment of sediment into suspension by a dense bottom current. *J. Geophys. Res.* 98, 4793–4807. doi: 10.1029/92JC02404

Goldhammer, R. K., Wickens, D. H., Bouma, A. H., and Wach, G. (2000). "Sequence stratigraphic architecture of the Late Permian Tanqua submarine fan complex, Karoo Basin, South Africa," in *Fine-Grained Turbidite Systems. American Association of Petroleum Geologists, Memoir*, eds A. H. Bouma and C. G. Stone (Tulsa, OK: SEPM, Special Publication), 165–172.

Groenenberg, R. M., Hodgson, D., Prélat, A., Luthi, S. M., and Flint, S. (2010). Flow-Deposit interaction in submarine lobes: insights from outcrop observations andrealizations of a process-based numerical model. *J. Sediment. Res.* 80, 252–267. doi: 10.2110/jsr.2010.028

Hansen, L. A. S., Callow, R. H. T., Kane, I., Gamberi, F., Rovere, M., Cronin, B. T., et al. (2015). Genesis and character of thin-bedded turbidites associated with submarine channels. *Mar. Pet. Geol.* 67, 852–879. doi: 10.1016/j.marpetgeo.2015.06.007

Haughton, P., Davis, C., McCaffrey, W. D., and Barker, S. P. (2009). Hybrid sediment gravity flow deposits – Classification, origin and significance. *Mar. Pet. Geol.* 26, 1900–1918. doi: 10.1016/j.marpetgeo.2009.02.012

Haughton, P. D. W., Barker, S. P., and McCaffrey, W. D. (2003). 'Linked' debrites in sand-rich turbidite systems - origin and significance. *Sedimentology* 50, 459–482. doi: 10.1046/j.1365-3091.2003.00560.x

Hodgetts, D., Drinkwater, N. J., Hodgson, J., Kavanagh, J., Flint, S., Keogh, K. J., et al. (2004). Three-dimensional geological models from outcrop data using digital data collection techniques: an example from the Tanqua Karoo depocentre, South Africa. *Geol. Prior Inf. Informing Sci. Eng.* 239, 57–75. doi: 10.1144/GSL.SP.2004.239.01.05

Hodgson, D. (2009). Distribution and origin of hybrid beds in sand-rich submarine fans of the Tanqua depocentre, Karoo Basin, South Africa. *Mar. Pet. Geol.* 26, 1940–1956. doi: 10.1016/j.marpetgeo.2009.02.011

Hodgson, D., Flint, S., Hodgetts, D., Drinkwater, N., Johannessen, E., and Luthi, S. (2006). Stratigraphic evolution of fine-grained submarine fan systems, Tanqua Depocenter, Karoo Basin, South Africa. *J. Sediment. Res.* 76, 20–40. doi: 10.2110/jsr.2006.03

Hodgson, D. M., Di Celma, C. N., Brunt, R. L., and Flint, S. S. (2011). Submarine slope degradation and aggradation and the stratigraphic evolution of channel–levee systems. *J. Geol. Soc.* 168, 625–628. doi: 10.1144/0016-76492010-177

Hofstra, M., Hodgson, D., Peakall, J., and Flint, S. (2015). Giant scour-fills in ancient channel-lobe transition zones: formative processes and depositional architecture. *Sediment. Geol.* 329, 98–114. doi: 10.1016/j.sedgeo.2015.09.004

Hofstra, M., Pontén, A. S. M., Peakall, J., Flint, S., Nair, K. N., and Hodgson, D. (2017). The impact of fine-scale reservoir geometries on streamline flow patterns in submarine lobe deposits using outcrop analogues from the Karoo Basin. *Pet. Geosci.* 23, 159–176. doi: 10.1144/petgeo2016-087

Hunter, R. E. (1977). Terminology of cross-stratified sedimentary layers and climbing-ripple structures. *J. Sediment. Res.* 47, 697–706.

Ito, M. (2008). Downfan transformation from turbidity currents to debris flows at a channel-to-lobe transitional zone: the lower pleistocene Otadai Formation, Boso Peninsula, Japan. *J. Sediment. Res.* 78, 668–682. doi: 10.2110/jsr.2008.076

Jobe, Z. R., Lowe, D., and Morris, W. (2012). Climbing-ripple successions in turbidite systems: depositional environments, sedimentation rates and accumulation times. *Sedimentology* 59, 867–898. doi: 10.1111/j.1365-3091.2011.01283.x

Johnson, S., Flint, S., Hinds, D., and De Ville Wickens, H. (2001). Anatomy, geometry and sequence stratigraphy of basin floor to slope turbidite systems,

Tanqua Karoo, South Africa. *Sedimentology* 48, 987–1023. doi: 10.1046/j.1365-3091.2001.00405.x

Jolly, R. J. H., and Lonergan, L. (2002). Mechanism and controls on the formation of sand intrusions. *J. Geol. Soc. London* 159, 605–617. doi: 10.1144/0016-764902-025

Kane, I., and Hodgson, D. (2011). Sedimentological criteria to differentiate submarine channel levee subenvironments: exhumed examples from the Rosario Fm. (Upper Cretaceous) of Baja California, Mexico, and the Fort Brown Fm. (Permian), Karoo Basin, S. Africa. *Mar. Pet. Geol.* 28, 807–823. doi: 10.1016/j.marpetgeo.2010.05.009

Kane, I., Kneller, B., Dykstra, M., Kassem, A., and McCaffrey, W. D. (2007). Anatomy of a submarine channel–levee: an example from Upper Cretaceous slope sediments, Rosario Formation, Baja California, Mexico. *Mar. Pet. Geol.* 24, 540–563. doi: 10.1016/j.marpetgeo.2007.01.003

Kane, I., and Pontén, A. S. M. (2012). Submarine transitional flow deposits in the Paleogene Gulf of Mexico. *Geology* 40, 1119–1122. doi: 10.1130/G33410.1

Kane, I., Pontén, A. S. M., Vangdal, B., Eggenhuisen, J., Hodgson, D., and Spychala, Y. T. (2017). The stratigraphic record and processes of turbidity current transformation across deep-marine lobes. *Sedimentology* 64, 1236–1273. doi: 10.1111/sed.12346

King, R. C., Hodgson, D., Flint, S., Potts, G. J., and Van Lente, B. (2009). Development of subaqueous fold belts as a control on the timing and distribution of deepwater sedimentation: an example from the southwest Karoo Basin, South Africa. *Extern. Control. Deep. Depos. Syst.* 91, 261–278. doi: 10.2110/sepmsp.092.261

Kneller, B., and Branney, M. (1995). Sustained high-density turbidity currents and the deposition of thick massive sands. *Sedimentology* 42, 607–616. doi: 10.1111/j.1365-3091.1995.tb00395.x

Komar, P. (1971). Hydraulic jumps in turbidity currents. *Geol. Soc. Am. Bull.* 82, 1477–1488. doi: 10.1130/0016-7606197182

López-Gamundí, O. R., and Rossello, E. A. (1998). Basin fill evolution and paleotectonic patterns along the Samfrau geosyncline: the Sauce Grande basin–Ventana foldbelt (Argentina) and Karoo basin–Cape foldbelt (South Africa) revisited. *Geol. Rundschau* 86, 819–834. doi: 10.1007/s005310050179

Lowe, D. (1982). Sediment gravity flows; II, Depositional models with special reference to the deposits of high-density turbidity currents. *J. Sediment. Petrol.* 52, 279–297.

Luthi, S. M., Hodgson, D., Geel, C. R., Flint, S., Goedbloed, J. W., Drinkwater, N. J., et al. (2006). Contribution of research borehole data to modelling fine-grained turbidite reservoir analogues, Permian Tanqua-Karoo basin-floor fans (South Africa). *Pet. Geosci.* 12, 175–190. doi: 10.1144/1354-079305-693

Macdonald, H. A., Peakall, J., and Wignall, P. B. (2011). Sedimentation in deep-sea lobe-elements: implications for the origin of thickening-upward sequences. *J. Geol. Soc. London* 168, 319–331. doi: 10.1144/0016-76492010-036

Marini, M., Felletti, F., Milli, S., and Patacci, M. (2016). The thick-bedded tail of turbidite thickness distribution as a proxy for flow confinement: examples from tertiary basins of central and northern Apennines (Italy). *Sediment. Geol.* 341, 96–118. doi: 10.1016/j.sedgeo.2016.05.006

Marini, M., Milli, S., Ravnas, R., and Moscatelli, M. (2015). A comparative study of confined vs. semi-confined turbidite lobes from the Lower Messinian Laga Basin (Central Apennines, Italy): implications for assessment of reservoir architecture. *Mar. Pet. Geol.* 63, 142–165. doi: 10.1016/j.marpetgeo.2015.02.015

Middleton, G., and Hampton, M. A. (1973). "Sediment gravity flows: mechanics of flow and deposition," in *Turbidites and Deep Water Sedimentation*, eds G. V. Middleton and A. H. Bouma (Tulsa, OK: Society of Economic Paleontologists and Mineralogists), 1–38.

Morris, E., Hodgson, D., Brunt, R., and Flint, S. (2014). Origin, evolution and anatomy of silt-prone submarine external levées. *Sedimentology* 61, 1734–1763. doi: 10.1111/sed.12114

Morris, E. A., Hodgson, D. M., Flint, S., Brunt, R. L., Luthi, S. M., and Kolenberg, Y. (2016). Integrating outcrop and subsurface data to assess the temporal evolution of a submarine channel-levee system. *AAPG Bull.* 100, 1663–1691. doi: 10.1306/04271615056

Morris, W., Scheihing, M., Wickens, D., and Bouma, A. H. (2000). "Reservoir architecture of deepwater sandstones: examples from the skoorsteenberg formation, Tanqua Karoo Sub-Basin, South Africa," in *Deep-Water Reservoirs of the World: GCSSEPM Foundation 20th Annual Research Conference*, eds P. Weimer, and M. Slatt, (Houston, TX: GCSSEPM Foundation), 629–666. doi: 10.5724/gcs.00.15.0629

Mutti, E., and Normark, W. (1987). "Comparing examples of modern and ancient turbidite systems: Problems and concepts," in *Marine Clastic Sedimentology*, eds J. Leggett and G. Zuffa (London: Graham and Trotman), 1–38.

Mutti, E., and Normark, W. (1991). "An integrated approach to the study of turbidite systems," in *Seismic Facies and Sedimentary Processes of Submarine Fans and Turbidite Systems*, eds P. Weimer and M. Link (New York, NY: Springer-Verlag), 75–106.

Nagatomo, A., and Archer, S. (2015). Termination geometries and reservoir properties of the Forties Sandstone pinch-out, East Central Graben, UK North Sea. *Geol. Soc. London, Spec. Publ.* 403, 133–155. doi: 10.1144/SP403.14

Oliver, M. A. (1990). Kriging: a method of interpolation for geographical information systems title. *Int. J. Geogr. Inf. Syst.* 4, 313–332. doi: 10.1080/02693799008941549

Patacci, M., Haughton, P., and McCaffrey, W. D. (2014). Rheological complexity in sediment gravity flows forced to decelerate against a confining slope, Braux, SE France. *J. Sediment. Res.* 84, 270–277. doi: 10.2110/jsr.2014.26

Pickering, K. T. (1981). Two types of outer fan lobe sequence, from the late Precambrian Kongsfjord Formation submarine fan, Finnmark, North Norway. *J. Sediment. Res.* 51, 1277–1286. doi: 10.1306/212F7E87-2B24-11D7-8648000102C1865D

Pierce, C. S., Haughton, P., and Shannon, P. M. (2018). Variable character and diverse origin of hybrid event beds in a sandy submarine fan system, Pennsylvanian Ross Sandstone Formation, western Ireland. *Sedimentology* 65, 952–992. doi: 10.1111/sed.12412

Porten, K., Kane, I., Warchol, M., and Southern, S. (2016). A sedimentological process-based approach to depositional reservoir quality of deep-marine sandstones: an example from the Springer Formation, Northwestern Vøring Basin, Norwegian Sea. *J. Sediment. Res.* 86, 1269–1286. doi: 10.2110/jsr.2016.74

Prélat, A., Covault, J. A., Hodgson, D., Fildani, A., and Flint, S. (2010). Intrinsic controls on the range of volumes, morphologies, and dimensions of submarine lobes. *Sediment. Geol.* 232, 66–76. doi: 10.1016/j.sedgeo.2010.09.010

Prélat, A., and Hodgson, D. (2013). The full range of turbidite bed thickness patterns in submarine lobes: controls and implications. *J. Geol. Soc. London* 170, 209–214. doi: 10.1144/jgs2012-056

Prélat, A., Hodgson, D., and Flint, S. (2009). Evolution, architecture and hierarchy of distributary deep-water deposits: a high-resolution outcrop investigation from the Permian Karoo Basin, South Africa. *Sedimentol.* 56, 2132–2154. doi: 10.1111/j.1365-3091.2009.01073.x

Pysklywec, R. N., and Mitrovica, J. X. (1999). The Role of Subduction-Induced Subsidence in the Evolution of the Karoo Basin. *J. Geol.* 107, 155–164. doi: 10.1086/314338

Richardson, J. F. (1971). "Incipient fluidization and particulate systems," in *Fluidization*, eds J. F. Davidson and D. Harrison (London: Academic Press), 25–64.

Rozman, D. J. (2000). "Characterization of a fine-grained outer submarine fan deposit, Tanqua-Karoo Basin, South Africa," in *Fine-Grained Turbidite Systems*, Vol. 72, eds A. H. Bouma and C. G. Stone (Tulsa, OK: AAPG Memoir), 291–298.

Satur, N., Hurst, A., Cronin, B. T., and Kelling, G. (2000). Sand body geometry in a sand-rich, deep-water clastic system, Miocene Cingoz Formation of southern Turkey. *Mar. Pet. Geol.* 17, 239–252. doi: 10.1016/S0264-8172(99)00005-7

Smith, R., and Joseph, P. (2004). Onlap stratal architectures in the Gres d'Annot: geometric models and controlling factors. *Geol. Soc.* 221, 389–399. doi: 10.1144/GSL.SP.2004.221.01.21

Smith, R. M. H. (1990). A review of stratigraphy and sedimentary environments of the Karoo Basin of South Africa. *J. Afr. Earth Sci.* 10, 117–137. doi: 10.1016/0899-5362(90)90050-O

Spychala, Y. T., Hodgson, D., and Lee, D. R. (2017a). Autogenic controls on hybrid bed distribution in submarine lobe complexes. *Mar. Pet. Geol.* 88, 1078–1093. doi: 10.1016/j.marpetgeo.2017.09.005

Spychala, Y. T., Hodgson, D., Prélat, A., Kane, I., Flint, S., and Mountney, N. (2017b). Frontal and lateral submarine lobe fringes: comparing sedimentary facies, architecture and flow processes. *J. Sediment. Res.* 87, 75–96. doi: 10.2110/jsr.2017.2

Spychala, Y. T., Hodgson, D., Stevenson, C., and Flint, S. (2017c). Aggradational lobe fringes: the influence of subtle intrabasinal seabed topography on sediment

gravity flow processes and lobe stacking patterns. *Sedimentology* 64, 582–608. doi: 10.1111/sed.12315

Stevenson, C., Jackson, C., Hodgson, D., Hubbard, S., and Eggenhuisen, J. (2015). Deep-water sediment bypass. *J. Sediment. Res.* 85, 1058–1081. doi: 10.2110/jsr.2015.63

Sullivan, M., Foreman, J. L., Jennette, D. C., Stern, D., Jensen, G. N., Goulding, F. J., et al. (2004). *Integration of Outcrop and Modern Analogs in Reservoir Modeling*, Vol. 80. Tulsa, OK: American Association of Petroleum Geologists Memoir, 215–234.

Sullivan, M., Jensen, G., Goulding, F., Jennette, D., Foreman, L., Stern, D., et al. (2000). *Deep-Water Reservoirs of the World*. Houston, TX: GCSSEPM Foundation, 1010–1031. doi: 10.5724/gcs.00.15.1010

Talling, P. (2013). Hybrid submarine flows comprising turbidity current and cohesive debris flow: deposits, theoretical and experimental analyses, and generalized models. *Geosphere* 9, 460–488. doi: 10.1130/GES00793.1

Talling, P., Masson, D., Sumner, E., and Malgesini, G. (2012). Subaqueous sediment density flows: depositional processes and deposit types. *Sedimentology* 59, 1937–2003. doi: 10.1111/j.1365-3091.2012.01353.x

Tankard, A., Welsing, H., Aukes, P., Newton, R., and Stettler, E. (2012). "Geodynamic interpretation of the Cape and Karoo basins, South Africa," in *Phanerozoic Passive Margins, Cratonic Basins and Global Tectonic Maps*, eds D. G. Roberts and A. W. Bally (Amsterdam: Elsevier), 869–894.

Tankard, A., Welsink, H., Aukes, P., Newton, R., and Stettler, E. (2009). Tectonic evolution of the Cape and Karoo basins of South Africa. *Mar. Pet. Geol.* 26, 1379–1412. doi: 10.1016/j.marpetgeo.2009.01.022

Twichell, D. C., Schwab, W. C., Nelson, C. H., Kenyon, N. H., and Lee, H. J. (1992). Characteristics of a sandy depositional lobe on the outer Mississippi fan from SEAMARC 1A sidescan sonar images. *Geology* 20, 689–692. doi: 10.1130/0091-7613(1992)020<0689:COASDL>2.3.CO;2

Van der Merwe, W. C., Hodgson, D. M., Brunt, R. L., Flint, S. S. (2014). Depositional architecture of sand-attached and sand-detached channel-lobe transition zones on an exhumed stepped slope mapped over a 2500 km^2 area. *Geosphere* 10, 1076–1093. doi: 10.1130/GES01035.1

Veevers, J. J., Cole, D. I., and Cowan, E. J. (1994). "Southern Africa: Karoo Basin and Cape Fold Belt," in *Permian- Triassic Pangean Basins and Fold Belts Along the Panthalassan Margin of Gondwanaland*, Vol. 184, eds J. J. Veevers and C. M. Powekk (Boulder, CO: Geological Society of America), 223–279. doi: 10.1130/MEM184-p223

Visser, J. N. J. (1997). Deglaciation sequences in the Permo- Carboniferous Karoo and Kalahari basins of the southern Africa: a toll in the analysis of cyclic glaciomarine basin fills. *Sedimentology* 44, 507–521. doi: 10.1046/j.1365-3091.1997.d01-35.x

Visser, J. N. J., and Praekelt, H. E. (1996). Subduction, mega-shear systems and Late Palaeozoic basin development in the African segment of Gondwana. *Geol. Rundschau* 85, 632–646. doi: 10.1007/BF02440101

Walker, R. (1978). Deep-water sandstone facies and ancient submarine fans: models for exploration for stratigraphic traps. *Am. Assoc. Pet. Geol. Bull.* 62, 932–966. doi: 10.1306/C1EA4F77-16C9-11D7-8645000102C1865D

Wickens, H., and Bouma, A. (2000). *The Tanqua Fan Complex, Karoo Basin, South Africa - Outcrop Analog for Fine-Grained, Deepwater Deposits*, Vol. 68. Tulsa, OK: SEPM Spec. Publ., 153–164.

Wild, R., Flint, S., and Hodgson, D. (2009). Stratigraphic evolution of the upper slope and shelf edge in the Karoo Basin, South Africa. *Basin Res.* 21, 502–527. doi: 10.1111/j.1365-2117.2009.00409.x

Wynn, R., Piper, D., and Gee, M. (2002). Generation and migration of coarse-grained sediment waves in turbidity current channels and channel–lobe transition zones. *Mar. Geol.* 192, 59–78. doi: 10.1016/S0025-3227(02)00549-2

Conflict of Interest Statement: AP was employed by the company Equinor ASA.

The remaining authors declare that the research was conducted in the absence of any commercial or financial relationships that could be construed as a potential conflict of interest.